# Driving Towards Efficiency

## Development of a Live Telemetry System and Driver Interface for UCL Shell Eco Marathon

**Team Members:**

Eric Hsieh

August Jaubert

Sándor Ötvös

Albert Cristian Tănase

Jahanzeb Zahid

**Supervisor:**

Dr. Llewellyn Morse

# Acknowledgements

We would like to express our gratitude to our project supervisor, Dr. Llewellyn Morse, for the continuous support throughout the project. His guidance shaped our work ethic to ensure the success of the project. His curiosity and enthusiasm made for exciting meetings and wonderful company. We will cherish the memories created together long past the end of our studies. We would like to thank the teaching staff and our peers at MechSpace for sharing their technical expertise that allowed us to develop a robust product, in particular William Backhouse for his help in developing the electrical circuits. We had a harmonious collaboration with the UCL Shell Eco-Marathon team who integrated us into their family with great warmth. Their help in arranging testing and understanding of the vehicle were key contributors to the project's development. Last but not least, we would like to thank our families, for their ongoing love and support that allowed us to chase our dreams.


# Abstract


This thesis presents the development of a novel telemetry system designed for an ultra-efficient vehicle competing in the Shell Eco-Marathon. The main goal of the competition is to complete a set number of laps within a given time. The car that manages to do so while using the least amount of energy is declared the winner. The telemetry system aims to provide a platform to record, store and evaluate the prototype's performance in real time and post-race. The data is transmitted over the bus using a CAN protocol, a racing and automotive standard.

The competition car is subject to design and component changes. As a result, the design process focused on expendability, user-friendliness and robustness, while ensuring cost-effectiveness and energy efficiency. To accommodate these criteria, a modular telemetry system was created, which allows for a rapid and easy integration of additional sensors. The electrical losses and weight of the system were reduced through an iterative process. The development emphasised careful consideration of components with minimal electrical expenditure and high performance. The reduction in circuit size and casing weight was accomplished through custom conformal designs of PCBs and component housings which facilitated the ease of use and robustness of the system.

A telemetry system is meaningful as long as the data can be evaluated and understood by the users. The innovative solution shifts the focus from speed-orientated optimisation, present in the racing industry, to the identification of patterns that lead to the minimisation of energy consumption. As a result, live and post-race analysis platforms have been developed for visualising and interpreting the data. This will aid driver training and the development of the car through three main data streams. The live incoming sensor information is displayed to the driver on an LCD screen which summarises the lap-by-lap performance. In depth data is sent to the race engineer using wireless communication, who will guide the driver in his race performance. Finally, the stored data on the on-board SD-card will be used for analysis using MATLAB that will further deepen the understanding of the car.

The work presented was used by the UCL Eco-marathon team in their competition in France. The telemetry system provided support during powertrain changes and competition attempts. The insights gained from the data analysis and innovative use of live-interfaces were used to apply for Off-track Awards at the competition. The team scored 88/100 in the Data and Telemetry Award, the highest score at this year's competition. This was given for the team's novel solution in finding racing patterns that improved efficiency. On top of this, the insights into energy reduction through data analysis contributed to the UCL Shell Eco-marathon team winning the Carbon Footprint Reduction Award. This performance provided an excellent evaluation of how the project team's design solution satisfied the requirements of the identified functions, objectives and constraints.


# Declaration

The team confirms that the work presented in this report is our own. Where information has been derived from other sources, we confirm that this has been indicated in the report.

# Contents

# List of Figures

# List of Tables

# 1 Introduction


Figure 1: UCL Shell Eco-Marathon Team winning the Data and Telemetry Award at Nogaro Circuit 2023.

## 1.1 Project Description and Previous Work

Shell Eco-Marathon is an international competition where teams are tasked with designing, building, and testing energy-efficient vehicle prototypes. The teams can compete in one of three categories: combustion engine, hydrogen, and battery electric. The objective is to complete a specific number of laps within a timeframe while consuming the least amount of fuel. In 2024, The European and African Eco-Marathon race will be held in Southern France on the Nogaro Circuit. Over 140 teams from the United Kingdom, France, Germany, Hungary, Bulgaria and Morocco bring their prototypes to compete against each other. The efficiency race will require the completion of 10 laps within 38 minutes. University College London is taking part in the Hydrogen class for the first time in 5 years.

The team's first participation was in 2015. The challenge of having a hydrogen powered chassis presented many obstacles throughout the years. Prior to the COVID-19 pandemic, the closest University College London got to completing a marathon race was in 2019, when a tyre puncture on the last lap denied the team from the first valid competition run. After the pandemic, new students have taken-up the project to bring it up to new heights. Last year's performance was the best to date in the team's history. Not only did University College London complete their first valid marathon run, but also came out on top of all other UK-based teams in the Battery Electric Class (including the likes of Imperial College London and University of Strathclyde). On top of this, the team's greatest achievement was winning the Data and Telemetry Award for developing a novel approach to determine the ideal race strategy that minimises energy consumption using a MATLAB simulation.

However, despite the success, the 2023 season highlighted several areas of improvement. During testing, the team identified limitations in the simulation algorithm. The driver had difficulties following the proposed ideal strategy. Moreover, the team had no means of validating the results of the simulation, as there was no system to record the car's velocity and position to allow for comparison between computational and real results. To overcome these limitations, this project aims to further innovate on previous season's work by developing a novel telemetry system and visualisation platforms that mitigate these issues. The system would offer real-time feedback to both the team and the driver, providing detailed information on the car's location, fuel consumption and velocity. This innovative approach will enhance the driver's guidance through a live on-board interface and improve the team's understanding of the car's energy losses. These are crucial in driving the development of the car towards success. On top of this, the design considerations emphasise UCL's sustainability goals that prioritise waste reduction through recyclability and long life cycles [1]. The work presented in this report was used to apply for the Data and Telemetry Award and contributed to the Carbon Reduction Footprint Award submission.

### 1.2 Report Structure

The report starts by describing previous work of UCL teams on telemetry. This is followed by a literature review to understand the background and existing solutions. This is used to determine the problem statement. Once the problem is understood, the FOCs (Functions, Objectives, Constraints) are defined, allowing for the formulation of the problem solution. With that in mind, the team's methodology is described and the design process for each subsection is detailed. This is followed by an evaluation of the subparts via testing and simulations. Finally, the entire system is assembled and tested. The solution is assessed against the previously defined FOCs, highlighting the strengths and weaknesses of the project. The report concludes with a future work section, discussing solutions to address current design shortcomings.

## 2 Background

### 2.1 History of UCL's Shell Eco-Marathon Team

To understand the current state of the UCL Eco-marathon team, it is important to briefly examine the history of the team. Previous research into data gathering and analysis has been conducted to estimate the car's acceleration profile and energy losses. The earliest investigation into the matter was done in 2015 [2]. A series of microcontrollers were attached to read parameters from the prototype's motor, fuel cell, supercapacitors, and throttle. This information was then displayed to the driver on an LCD screen. However, the data was not stored externally, making post-race analysis of the prototype impossible.

Further developments were achieved in 2017 [3]. An operational amplifier was installed to reduce electrical noise of the readings. An RTC (Real Time Clock) and SD card module were added to record data. Finally, a GPS module was also installed to keep track of the prototype's position and velocity around the track. This system was capable of measuring fuel cell and supercapacitor voltage along with velocity and distance travelled. This allowed the team to relate the car's power output with the on-track geographical profile. Some of this data was shown to the driver through an LCD screen.

Final developments were done by the team in 2019 [4]. Most previous efforts had stagnated in favor of performance studies. Research was performed to simulate and optimise fuel consumption of the vehicle. Additionally, a temperature sensor was added to monitor fuel cell efficiency and Hall-effect sensors were mounted to the break disks to monitor hydraulic brake defects.

Covid-19 disrupted any continuation on development of telemetry and data visualisation systems. Moreover, after the pandemic, none of the previous work or systems were passed down to the newly formed team. This leaves the members without any means of evaluating their car's efficiency, nor the driver's ability to reduce fuel consumption. This is hampering the team's performance prospects in the 2024 race. In the coming Shell Eco-marathon competition, UCL will be the only UK team running on hydrogen. Given this year's focus on developing a new hydrogen powertrain, there is an urgent need to develop a novel telemetry system and performance analysis platform to ensure safe and efficient progress.

This report presents an innovative approach to overcoming the shortcomings of previous telemetry systems by developing new methods for guiding the driver and car development. By introducing cutting-edge techniques and design choices, we have created a live telemetry system and data analysis platforms that not only meet current needs but also ensure ease of use and comprehensive documentation. This will enable the UCL Shell Eco-Marathon team to continue using the platform in future competitions, setting a new standard for telemetry systems in the context of hydrogen-powered vehicles.

### 2.2 Introduction to Telemetry and Vehicle Data Analysis

To define the problem solution, it's essential to understand how a vehicle's efficiency can be analysed, which requires the collection and processing of data. One of the most important weapons for a race car team is information. Information gives racing teams insight into the performance characteristics of the vehicle and the driver in real-time and after the race. The subsequent analysis of this information leads to better racing performance and a higher rate of improvement [5]. A system capable of acquiring race data, storing it, and or transmitting it is called a telemetry system.

### 2.2.1 Data Acquisition

Data acquisition is conducted via sensors. Sensors can be classified into three groups depending on their functionality. Control sensors, which replace traditional mechanical controls of a vehicle, enhancing precision. Monitoring sensors, which monitor the health of the vehicle to prevent failure and ensure safety. Finally, instrumentation sensors, which are used to gather information about the vehicle's environment and performance. This is the category that is most frequently used for data analysis [6].

In a vehicle data gathering system, a large combination of sensors are used in tandem. Communication between various sensors is usually necessary and done via a network. A node can be defined as a member of the network that can take measurements, process data, and communicate with other devices connected to the network. The network topology will determine how the nodes interact with each other. Automotive applications most commonly utilise a bus, star, ring, or a combination of these known as a hybrid topology. It is important to note that no single topology is ideal for every application. Instead, each is suited to a specific set of applications [7]. Table 1 summarises the strengths and weaknesses of the various topologies.

Table 1: Automotive network topology pros, cons, and protocols.

| Topology | **Bus** | **Star** | **Ring** | **Hybrid** |
|---|---|---|---|---|
| Pros | Scalable<br>Cost-effective | Easy management<br>Scalable | Fast data transfer<br>Equal network access | Flexible<br>Scalable |
| Cons | Limited bandwidth<br>Troubleshooting | Expensive<br>Central failure point | Prone to failure<br>Hard to modify | Complex<br>Expensive |
| Protocols | CAN [8] | FlexRay [9] | Token Ring [10] | MOST [11] |

**Bus topology:** Bus topologies utilise a single communication line, known as a bus, to transmit data. On this network, an arbitrary number of nodes can be attached via cables. This makes the system scalable and cost-effective. Due to the nature of the topology, only a single message can be sent at any point in time. Hence, a queuing system must be implemented that handles each node's access to the bus. Consequentially, as the network expands, the amount of time each node has to send a message decreases, making the network easily congested and hard to troubleshoot. The other drawback of such a system is that if the bus fails, all communication is compromised [12]. The most commonly used bus protocol in automotive applications is the CAN (Control Area Network) protocol [8].

**Star topology:** A star topology has two components, a central switch and nodes that are all directly connected to the switch but not to each other. The central switch acts as the server by managing the flow of information between nodes. The advantages of such a network are that it can entirely be managed via the switch, and it is easily scalable. However, the failure of the central switch will result in the failure of the entire network [12].

**Ring topology:** Ring topologies work by creating a link between a node and the two nodes neighbouring it, forming a ring of connections. Two-way communication can be achieved by creating a second ring, making the system more robust. This results in fast data transfers while allowing each node to be a sender and receiver simultaneously. However, the failure of a single node will compromise the entire network and adding nodes requires the system to be shut down [12].

**Hybrid topology:** A hybrid topology can be formed by combining any of the previously mentioned topologies together. Such topologies are most commonly found in medium to large scale applications, where each sub network has a topology that best matches its use case. The advantages and disadvantages of such networks depend on the type of networks that have been merged [12].

**Vital parameters of a vehicle:** There is almost a sensor for every application, hence it is important to list the most vital parameters that should be measured if a data gathering system is to be implemented. These parameters are the engine RPM, wheel speed, throttle position, steering angle, and lateral and longitudinal acceleration [13]. Knowledge of these parameters enables performance analysis of the vehicle.

**Engine RPM and wheel speed:** Both engine RPM and wheel speed are measured in the same way; by relating the rotation of the crankshaft or the wheel to a potential difference which is easier to measure. This is commonly done by Hall effect and inductive sensors. Both of these sensors measure the frequency of the alternating voltage signal induced by the rotation of the wheel [14, 15].

**Throttle position and steering angle:** A potentiometer can be used to monitor the angle of the throttle and the steering wheel. This is based on how much the throttle is depressed, or the wheel is rotated by the driver, altering the measurement of the voltage. This can then be correlated to obtain the angle value and hence the position [16].

**Lateral and longitudinal acceleration:** Acceleration can be measured by an accelerometer, such as a micro-electromechanical systems accelerometer, which is a 3-axis device that records acceleration in X, Y, and Z directions [17]. Sensors that measure speed, such as the Hall-effect sensor, can also be used to determine acceleration.

### 2.2.2 Data Storage and Transmission

Once all the sensors have been connected to the network, the readings need to be stored, for post-race analysis, and transmitted for real-time data analysis.

**Onboard data storage:** Onboard storage is accomplished by connecting a storage device to the system, which saves sensor readings throughout the race.

**Offboard data storage:** Offboard data storage requires data to be transmitted from the vehicle to the storage solution. This necessitates the use of wireless communication. Wireless communication protocols can be grouped into WLAN (Wireless Local Area Networks) and WWAN (Wireless Wide Area Networks) [18]. Table 2 highlights the main advantages and disadvantages of such networks. Furthermore, unlicensed wireless network solutions are associated with WLAN, making them cheaper but less secure and more susceptible to interference. While WWAN usually employs licensed networks, making them safer and more reliable when transmitting data, they require a service fee to use [18].

Table 2: WLAN and WWAN wireless communication protocol's pros, cons, and examples.

| Protocol | **WLAN** | **WWAN** |
|---|---|---|
| Pros | Cheap<br>High data speeds | High coverage<br>High range |
| Cons | Limited range<br>Requires local infrastructure | Expensive<br>Requires external service provider |
| Examples | Bluetooth, Wi-Fi, Zigbee | Cellular, LoRaWAN |

**Communication protocols:** Zigbee utilises unlicensed frequencies to achieve wireless communication. It is a low power, low cost, and low range solution. Due to this, its main area of application is battery powered devices [19].

Cellular protocols were developed with M2M (Machine-to-Machine) communication in mind. It has data encryption via IPsec (Internet Protocol Security) and VPN (Virtual Private Network). Depending on the version being used, it can send large amounts of data at great speeds, however the technology is expensive to implement or requires service providers to use [20]. Fortunately, such networks have been deployed throughout the world, making the technology easily accessible [21].

LoRaWAN is an example of a WWAN protocol which can utilise both the unlicensed and licensed radio spectrums based on the required application. It is capable of low power and low data communication over a large distance. It also uses a 1% radio duty cycle, meaning it can only transmit data for 1% of its operational time. It is mainly used for applications that are not latency sensitive [18].

### 2.2.3 Data Analysis

The previous sections detailed how to collect, store and transmit data of a race car, enabling data analysis. However, whatever the price of the data acquisition system, it is inefficient use of money if the recorded data is not interpreted correctly [5]. Over a typical race, vehicles equipped with a telemetry system will transmit around 3 GB of data, along with logging a further 4 GB. Once this raw data is processed and combined with other data streams such as video and audio, the resulting data usually exceeds 1 terabyte in size [6]. Various methods have been developed to help visualise this excessive amount of data in a meaningful way.

Data analysis usually involves overlaying multiple lap plots of various sensor readings against distance or time and identifying patterns. For example, overlaying speed plots allows for the comparison of different driving styles and drivers. The main things to look out for are the differences between the height of the peaks and valleys along with the curvature of the lines between them. This indicates the race line taken [13]. Besides plots, histograms and report tables can also be used to further the analysis of the vehicle's and driver's performance.

### 2.2.4 Current Telemetry Systems

Currently available systems for vehicle applications incorporate all the aforementioned features. These systems focus on gathering data to enhance race performance by minimizing lap times. Typically, the data logging system in a vehicle weighs between 0.8-1.2kg and consumes 5-12W of power (Table 3).

Table 3: Off-the-shelf telemetry system power usage and weight.

| **System** | **Dx-telemetry** [22] | **VG710** [23] | **Tel2 Race Car Telemetry** [24] |
|---|---|---|---|
| **Power Usage (W)** | $< 5$ | 12 | 10 |
| **Weight (g)** | 800 | 775 | 1210 |

## 2.3 Problem Statement

Currently, there are no means of evaluating the Shell Eco marathon team's vehicle and driver performance, hindering the rate of future improvements. The competition's objective is to maximise energy efficiency, requiring an in depth understanding of how the electrical, mechanical, and human aspects interact and influence performance. Knowledge of the interplay between these variables will allow the team to minimise energy consumption during the race, hence maximising the chances of success.

Existing telemetry systems are designed for consumer vehicles weighing over a tonne. In contrast, the Shell Eco-marathon car weighs only 45kg. Implementing these existing solutions would drastically decrease the car's energy efficiency. The combination of these factors makes off-the-shelf solutions unsuitable for the marathon car.

# 3 Engineering Problem Requirements

Now that the problem is understood, the solution can be outlined. This can be done by defining the FOCs that the system must meet. This ensures that the solution is of a high quality while addressing the issues mentioned in the problem statement. Furthermore, the team's design philosophy is outlined, which is the backbone of how design problems are approached and evaluated.

## 3.1 FOCs and Design Thinking

HOQ (House of Quality) analysis was used to determine the FOCs of the project. This allowed the team to approach the problem from the user's point of view and identified key aspects of the project.

**House of quality analysis:** House of quality analysis starts with determining the users' wants of the product. These wants are purposefully vague. A good example of a want is 'cheap'. These wants are then elaborated upon by the engineer to create a more specific description. For the want of 'cheap' an engineering description would be 'cheaper than current products on the market that offer similar functionalities'. Once both sides have been defined,

they can be compared with each other to create a ranking. Characteristics with a higher ranking should be prioritised, since they produce more value for the user. This ranking also served as a management tool for the team, by focusing on high priority characteristics it could be ensured that the team is placing most of its focus on key aspects.

Since the design team and the user are not the same, it is possible the requirements that the team specified are not representative of the users' needs. To minimise this risk, the team took an iterative approach in defining the characteristics. This was then followed by discussions with the Shell Eco marathon team, who are the users, to get their input. This approach allowed for the completion of the HOQ analysis which is representative of both the user and the engineers (Fig. 2).

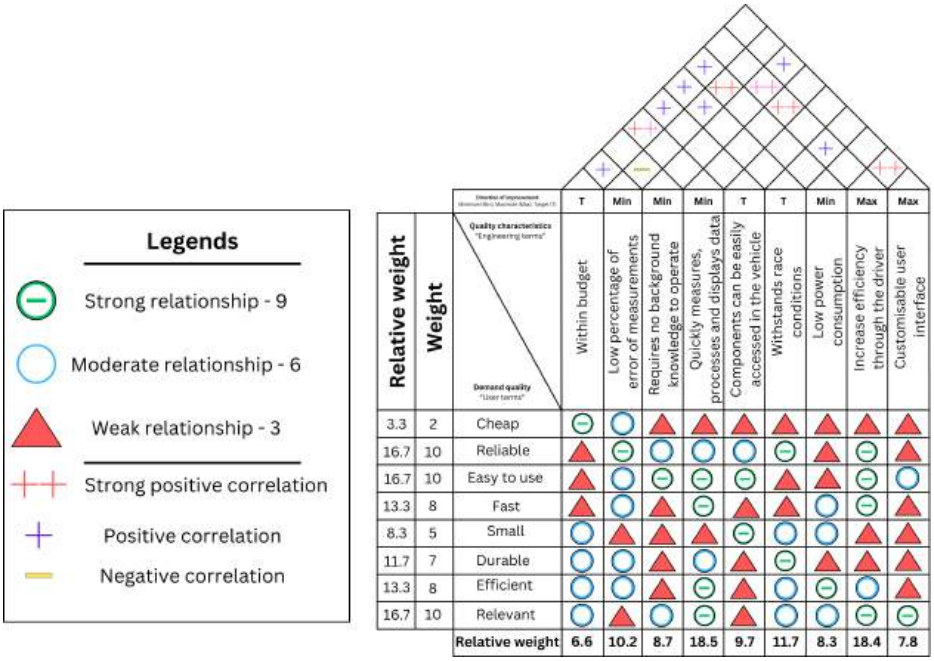


Figure 2: House of quality analysis table.

**Functions, objectives, and constraints:** Table 4 shows the characteristics ranked based on their weighting. Based on this analysis, the aim of the project should be to develop a system that is capable of consistent data measurement throughout the race, enabling the driver to improve.

Table 4: HOQ analysis results.

| **Characteristic** | **Weight** | **Rank** |
|---|---|---|
| Quickly measures, processes, and displays data | 18.5 | 1 |
| Increase efficiency through the driver | 18.4 | 2 |
| Withstands race conditions | 11.7 | 3 |
| Low percentage error of measurements | 10.2 | 4 |
| Components easily fit in the vehicle and can be easily removed | 9.7 | 5 |
| Requires no background knowledge to operate | 8.7 | 6 |
| Low power consumption | 8.3 | 7 |
| Customisable user interface (to change the layout) | 7.8 | 8 |
| Within budget | 6.6 | 9 |

With the HOQ analysis in mind, the FOCs were created. They focus on what a functioning system should be able to do and are grouped based on the functions (Table 5). Justifications, where applicable for each constraint, are mentioned after Table 5.

Table 5: Functions, Objectives, Constraints.

| Function | Objective | Constraint |
|---|---|---|
| **1.0** Data Collection | **1.1.0** Collect relevant data | **1.1.1** All quantities relevant to performance are measured |
| | **1.2.0** Accurate measurements | **1.2.1** Measurement accuracy is within 5% of the actual value |
| | **1.3.0** Prompt measurements | **1.3.1** At least 1 new measurement per second |
| | **1.4.0** Reliable measurements | **1.4.1** The output range for same inputs is within 5% |
| **2.0** Data Transmission | **2.1.0** System sends relevant data | **2.1.1** The relevant data is transmitted to separate interfaces |
| | **2.2.0** Wireless communication | **2.2.1** Data can be sent wirelessly throughout the track |
| | **2.3.0** Continuous data feed into the interfaces | **2.3.1** Data is sent every time a new measurement is processed |
| | | **2.3.2** The data is not delayed more than 200 milliseconds |
| | **2.4.0** Error detection of miscommunication | **2.4.1** Unsuccessful message transfer can be identified |
| | | **2.4.2** Message transfer probability > 90% |
| **3.0** Data Processing | **3.1.0** Raw data decoding | **3.1.1** Raw sensor measurement format |
| | **3.2.0** Prompt data processing | **3.2.1** Raw sensor data should not stockpile |
| | **3.3.0** Low computational intensity | **3.3.1** Processing can be done with microcontrollers |
| **4.0** Data Storage | **4.1.0** Data is stored permanently | **4.1.2** The data is not lost if the storage device is powered off |
| | **4.2.0** Data is easy to access | **4.2.1** Intuitive file structure |
| | **4.4.0** Data can be written quickly | **4.4.1** Data storage does not impact processing times |
| **5.0** Data Visualisation | **5.1.0** Performance data is displayed reliably and accurately | **5.1.1** All necessary information is displayed simultaneously |
| | | **5.1.2** Displayed information is up-to-date |
| | **5.2.0** Interface is intuitive and easy to interpret | **5.2.1** The display layout adheres to the wants of the users |
| | | **5.2.2** Display does not compromise the user's safety |
| **6.0** System Design | **6.1.0** Easy to use | **6.1.1** System can easily be taken apart and assembled |
| | | **6.1.2** No ambiguities regarding its assembly |
| | **6.2.0** Easy to expand | **6.2.1** Developments have to be compatible with current system |
| | **6.3.0** Easy to manufacture | **6.3.1** Manufacturing requirements are easily available |
| | **6.4.0** Sustainable | **6.4.1** Can be recycled |
| | **6.5.0** Low weight | **6.5.1** System is lighter than 1kg |
| | **6.6.0** Low power consumption | **6.6.1** System uses less than 5W |
| | **6.7.0** Low-cost | **6.7.1** System costs < £2500 |
| | **6.8.0** Robust | **6.8.1** Components withstand race conditions |

**Data collection 1.1.1 and 1.3.1:** Based on the HOQ analysis, low percentage error of measurements is the 4th most important aspect of the project, hence a low tolerance for deviation of the actual value was specified.

**Data transmission 2.3.1 and 2.3.2:** The data transfer frequency can be determined using the vehicle's top speed, which is around 10 m/s. Sending a successful message every 200 ms ensures that the vehicle has moved a maximum distance of 2 m, making it relevant to the race engineer when received. To guarantee at least a 90% transfer probability within the 200 ms timeframe, multiple messages should be sent.

**System design 6.2.1, 6.3.1 and 6.4.1:** The system should minimise the use of materials, where possible. Thus, reducing the overall footprint of the system to conserve the limited space available in the vehicle and reduce its weight, thereby maintaining its efficiency. Emphasis will also be placed on reusing suitable components that are already available at MechSpace to reduce waste. The system should be compatible with future Shell Eco-marathon vehicles that the UCL team produces. It should be durable to prolong its lifespan. Components that have been damaged should be capable of being recycled, reducing their end of life environmental impact.

**System design 6.5.1 and 6.6.1:** Given Shell Eco marathon's focus on achieving energy efficiency, the developed system should be lighter while also using less power than off the shelf solutions, justifying its development.

### 3.2 Design Approach

The approach to this project is based on the Double Diamond diagram from the Design Thinking methodology (Fig. 3). The Discover and Define phases are used to guide the background research needed to articulate the problem statement into a form that is relevant to the given subsystems. This is followed by the Develop and Deliver phases resulting in the final design.

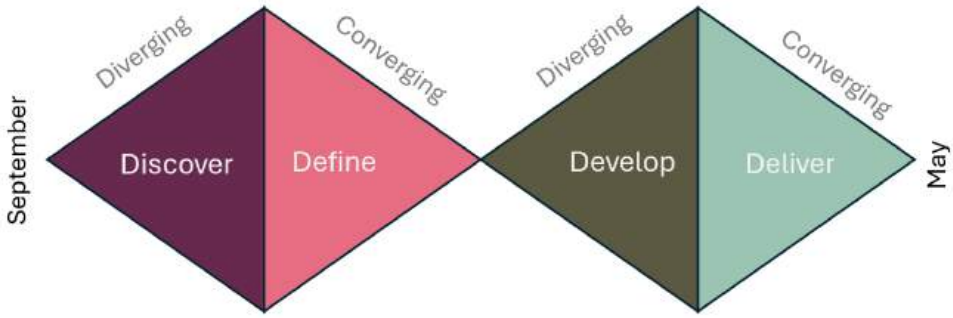


Figure 3: Stages of the double diamond showing the Design Thinking methodology.

It needs to be noted that this design process is highly iterative, allowing the team to further explore the problem space beyond the initial literature review. For example, during the Discover and Define phases, prototyping was crucial in understanding the capabilities and limitations of electronics, and user interviews helped define user focused features of the live driver interface. Only at this point was the project advanced to the Develop and Deliver phases. For instance, the electronics' casings were taken through several phases of concept generation and initial prototyping. This resulted in the final design selection and validation via a full system test at the CycloPark track in Greater London.

### 3.3 Problem Solution

To evaluate the vehicle's and driver's performance a telemetry and data analysis system will be developed that adheres to the requirements of the Shell Eco marathon competition. The system should continuously collect, store, and transmit relevant performance data. The data processing aspect will consist of real-time and post race data analysis. Real-time data analysis allows for the evaluation of the driver's performance during the race. It should be communicated to the driver and the race engineer simultaneously. The data communicated should be useful and easy to understand allowing for adjustments during the race. Post race data analysis is concerned with assessing the vehicle's performance, in greater depth, highlighting areas of improvement within the vehicle. The system should also be scalable and well-documented to ensure its usability by future UCL Shell Eco-marathon teams.

## 4 Methodology

This section documents how the team followed the outlined design approach throughout the project. Figure 4 shows the subsystems of the design. The four main parts are: electrical, system information, data visualisation, and casing. The electrical part is the backbone of the project, it describes how the physical electrical components were designed to be able to record, store, and transmit data. This section covers FOCs 1.0 Data Collection, 2.0 Data Transmission, 4.0 Data Storage, and 6.0 System Design. System information outlines how the recorded data propagates along the network to achieve data storage and transmission, covering FOCs beginning with 3.0 Data Processing and 4.0 Data Storage. Once information is available, the data visualisation section details how it is displayed to both the driver and race engineer, addressing FOCs relating to 5.0 Data Visualisation. Finally, casings were designed to protect the electrical components within the vehicle, with a focus on FOCs 6.0 System Design.

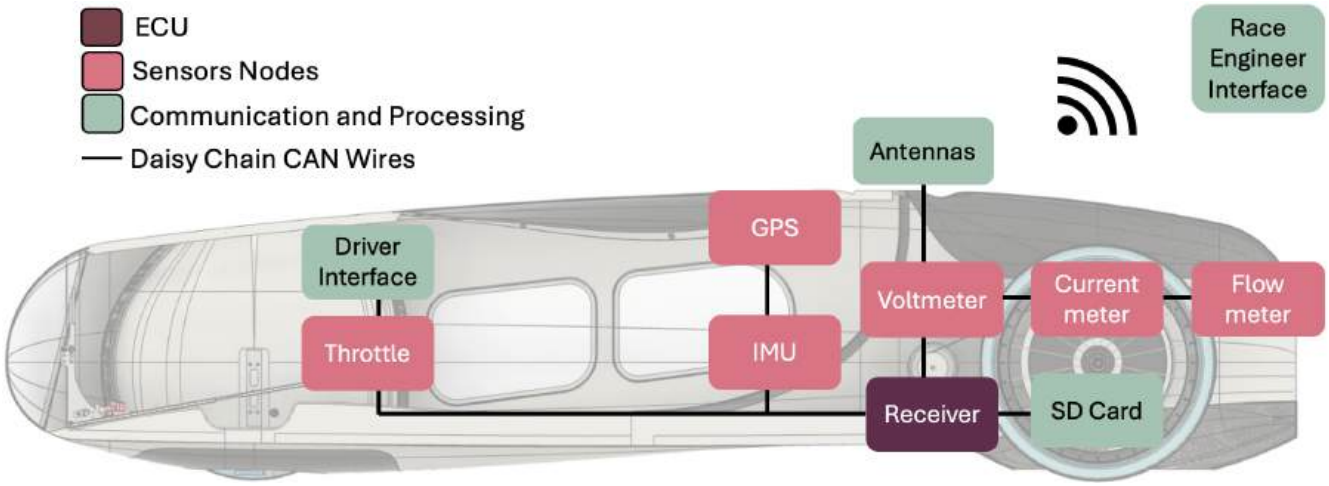


Figure 4: Proposed Telemetry System Schematic.

## 4.1 Electrical Circuits

### 4.1.1 Discover Phase

In the initial Discover phase, extensive research was done to identify the components that make up telemetry systems, identifying user needs, and using rapid prototyping with some technologies found from the literature review to better understand the technical requirements of the project.

**Preliminary research:** Fundamentally, a telemetry system encompasses sensors measuring their environment, controllers handling the data, a method for sharing digital information between controllers (i.e. a communication protocol), a method to log the sensed data, and a telecommunication technique, all of which necessitate careful consideration. A comprehensive list of potential technologies was curated, each aligned with the system's intended functions and objectives (Table 6).

Table 6: Technologies for Data Transmission, Processing and Storage.

| Function | Technologies |
|---|---|
| **2.0 Data Transmission** | **2.2.0 & 2.5.0: Long Range Wireless Communication**<br>- Frequency Modulated (FM) radio<br>- Broadband (4G)<br>- Satellite communication (Iridium, etc.) |
| **3.0 Data Processing** | **3.1.0: Data Conversion**<br>- Microcontroller (Arduino, STM32, etc.)<br>- Field-Programmable-Gate-Arrays (FPGA)<br>- Microprocessor (Raspberry Pi, etc.) |
| **4.0 Data Storage** | **4.1.0: Permanent Data Storage**<br>- Secure Digital (SD) card<br>- Non-volatile flash memory<br>- HDD / SSD |

**Rapid prototyping:** The initial prototyping phase commenced by repurposing existing sensors, microcontrollers, and radio transceivers sourced from previous projects found in UCL Mechspace, satisfying FOC 6.4.0. This included components such as the Bosch BNO055 sensor for the Inertial Measurement Unit (IMU), an Adafruit Ultimate GPS module for GPS functionality, Arduino Uno and Teensy development boards, NRF24+ radios, and CAN transceivers. These components formed the foundation for setting up a simplified telemetry system, facilitating the evaluation of standardized communication protocols like CAN, Inter-Integrated Circuit (I2C), and Serial Peripheral Interface (SPI).

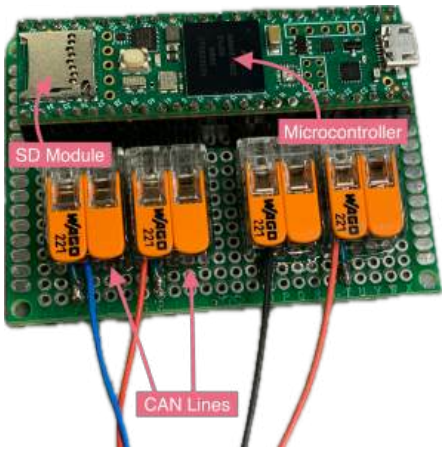


Figure 5: CAN to SD data-logger prototype.

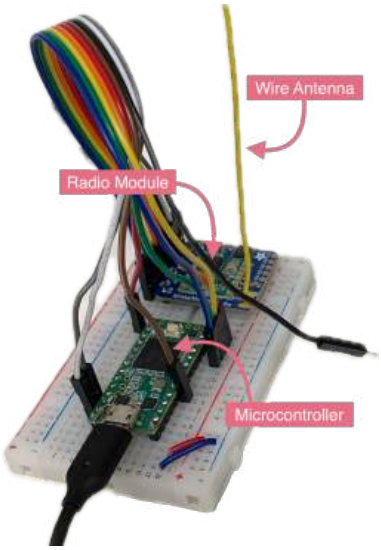


Figure 6: Radio communication test board.

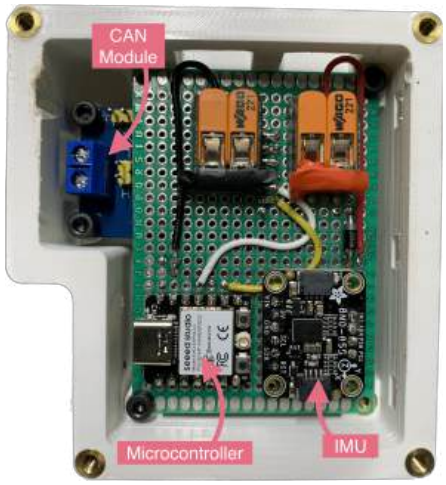


Figure 7: Sensor CAN node prototype.

The prototypes allowed for insights into the operational nuances of the hardware through hands-on testing. These focused on transferring sensor data, and transmission protocol robustness. This approach proved to be more effective compared to theory, especially in exploring transmission protocols, where various setups with varying hardware configurations and transmission data were tested. This allowed the team to better appreciate the complexities inherent in implementing data transmission and enhancing its ability to develop robust solutions.

### 4.1.2 Ideal Solution

Following this, the Define stage allowed these findings to be translated into precise design objectives, outlining the scope and goals of the telemetry system. The team proceeded to select components for the system, considering factors such as performance, reliability, cost, and availability.

**Sensors:** From discussions with the Shell Eco Marathon team and the literature review, it was determined that the system should be able to record position, acceleration, voltage, current and volumetric flow rate values. Satisfying FOC 1.1.0. Various sensors capable of measuring these quantities were tested. During rigorous testing, challenges were encountered with defective components, particularly with GPS and CAN transceivers, underscoring the criticality of sourcing high-quality components to ensure system reliability. This resulted in more emphasis being put on quality in the selection process, culminating in the following sensors and sampling frequencies being selected:

- **Position**: uBlox MAX-M10S (GNSS) (Procured), sampling frequency: 5Hz
- **Forces, acceleration**: Bosch BNO055 (IMU) (Re-utilised), sampling frequency: 100Hz
- **Voltage**: Texas Instrument ADS115 (Analog to Digital Converter) (Procured), sampling frequency: 2Hz
- **Current**: LEM HO 50-S/SP30 (Current Transformer) (Procured), sampling frequency: 2Hz

These sensors are capable of meeting the criteria outlined by FOCs 1.2.0, 1.3.0, and 1.4.0. This phase also brought to light a significant concern regarding the supply chain dynamics of electronic components essential for our project. The unpredictable availability of parts underscored the necessity for a solution that fosters adaptability. This highlighted the importance of the system being easily expandable to prolong the project's longevity and ensure its viability for future users (FOC 6.2.0 and 6.3.0).

**Controllers:** Following the selection of the sensors, focus was placed on identifying the ideal microcontroller. For this implementation an ideal microcontroller would be cost-effective and simple, while having the highest energy efficiency. Hence, the thorough selection of microcontrollers was conducted.

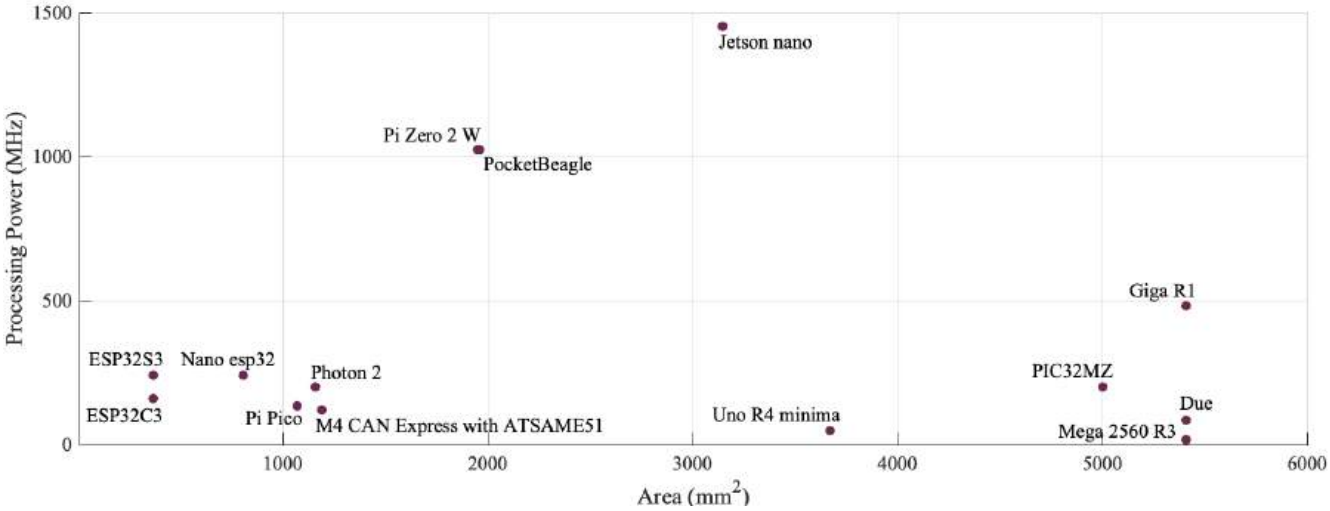


Figure 8: Microcontroller selection compared by size and processing power.


Figure 9: ESP32-C3 development board manufactured by Seeed.

After a meticulous evaluation of price, availability, speed and size (Fig. 8), Espressif microcontrollers were selected, specifically the ESP32-C3 and ESP32-S3 development boards by Seeed (Fig. 9). These boards, having identical footprints, offer seamless interchangeability, enhancing the flexibility of the system design. The ESP32-C3 stands out in setups prioritising energy efficiency, consuming approximately half the power of the ESP32-S3 (approximately 0.25 Watts), making it an ideal choice. Conversely, the ESP32-S3 offers accelerated processing with its two cores, higher clock speeds, and additional non-volatile flash memory storage, making it crucial for scenarios demanding faster processing and additional features such as native SD support. These attributes, bundled in a compact package, fit well within the defined requirements.

**Data storage:** After thorough evaluation, the team opted for microSD cards as a medium of data storage. Although during initial trials with SD data logging, an issue was encountered with slow write speeds, with each line of values taking approximately 400ms to save. Recognising the importance of efficient data logging, methods were explored to accelerate SD logging to optimise the system's performance. SD cards were selected due to their affordability, ease of access, sharing, and straightforward upgradeability. SD cards offer robustness against physical wear and tear, making them suitable for rugged environments. While flash storage may provide faster processing speeds, its lower storage capacity at a comparable cost rendered it less favourable. SD cards meet the requirements defined by FOC 4.0.

**CAN as the communication protocol:** Since communication is what links all the components of the system together, the selection of a suitable communication protocol is paramount to the system's success. Throughout the prototyping phase, the superiority of CAN over other protocols such as I2C and SPI became evident. CAN demonstrated greater resilience to unfavourable conditions, exhibiting lower sensitivity to noise and varying power levels. Its large network distance and support for asynchronous data sharing at high data rates further distinguished it as the optimal choice. By halving the number of messages on a bus for the same data rate (e.g. 125kbit/s) compared to other protocols, CAN minimised the likelihood of message interference, ensuring a more reliable and efficient data transmission. Additionally, CAN's asynchronous nature allowed sensors to transmit data autonomously, eliminating the need for sequential request and reception patterns typical of other protocols.

**Telecommunication:** Communication between the vehicle and the race engineer is crucial for real-time performance analysis. Wireless transmission emerges as the most suitable option. After a thorough evaluation, frequency-modulated radio communication is the preferred approach. Unlike broadband alternatives, radio communication

offers a cost-effective solution. However, it is important to acknowledge its limitations such as line-of-sight transmission challenges and susceptibility to obstacles. Frequency selection significantly impacts transmission performance; lower frequencies provide better obstacle penetration but may sacrifice data speed, while higher frequencies offer faster data rates, but are more prone to signal attenuation. Choosing the appropriate transmission frequency band was crucial. Following careful consideration, the 433MHz frequency band was selected from available options (433 MHz, 915 MHz, and 2.4 GHz). Its robust resistance to interference, coupled with satisfactory data transfer speeds of approximately 250 kbits/s based on initial calculations, aligns well with the project's needs (FOC 2.2.0). Furthermore, compliance with UK and EU regulations for non-specific short-range devices ensures both legal conformity and operational reliability. These design choices were later verified via testing (Section 5.2.1).

### 4.1.3 Developing the Solution

In the Develop phase, the aim was to translate the identified requirements into concrete solutions.

Table 7: Electrical circuit requirements.

| Requirement | Description |
|---|---|
| **Expandable (FOC** 6.2.0**)** | The system must be expandable, to accommodate new sensors, data channels, or functionalities without necessitating significant hardware or software overhauls. Ensuring scalability and adaptability to evolving project / user needs, technological advancements and component availability. |
| **Robust (FOC** 6.8.0**)** | The system should be resilient to various environmental conditions, mechanical and electrical misuses through protection mechanisms. Ensuring reliable operation in demanding situations, enhancing overall system performance and longevity. |
| **User-friendly (FOC** 6.1.0**)** | The interface and operation of the system must be intuitive and accessible to users with varying levels of technical expertise. This includes clear documentation, simplified setup procedures, and ergonomic design considerations to streamline configuration and maintenance tasks. |
| **Resource-efficient (FOC** 6.4.0**)** | The telemetry system should optimize power consumption and the mass of system components, to minimize impact on the vehicle's performance. |
| **Cost-effective (FOC** 6.7.0**)** | The design should be cost-efficient without compromising performance or reliability. This involves leveraging commercially available components, optimising manufacturing processes, and minimising maintenance requirements to ensure a favourable balance between upfront investment and long-term operational expenses. |

**Expandable:** To address the need for expandability, the telemetry system adopts a modular architecture, allowing seamless integration of additional sensors, data channels, or functionalities without requiring extensive hardware or software modifications. Central to this approach is the implementation of a CAN bus, facilitating communication between system components. Each system node is composed of two main elements: a sensor module and a computing unit. The computing unit serves as a versatile platform capable of interfacing with a wide range of sensors through standardised communication protocols such as I2C, SPI, and analogue voltage sensing.

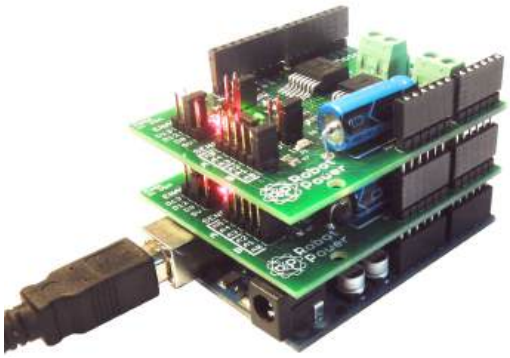

Figure 10: Two motor controller shields stacked on an Arduino Uno board.

To implement modularity, shields were created, similar to the ones commonly used in embedded systems, to extend the capabilities of the main computing unit (Fig. 10). It establishes a standardized connection blueprint between the computing unit and the sensor module, giving users a flexible platform to seamlessly integrate various sensors into the telemetry system. This approach enhances expandability by offering a fixed footprint and access to input/outputs (I/O) of common sensor communication protocols (I2C, SPI), empowering users to customize and expand the system according to their specific requirements.

In essence, this means creating an "Arduino-like" development board with straight access to necessary I/O pins, to fit the system specifications of user-friendliness, resource efficiency, robustness and cost-effectiveness (FOCs 6.1.0, 6.2.0, and 6.4.0).

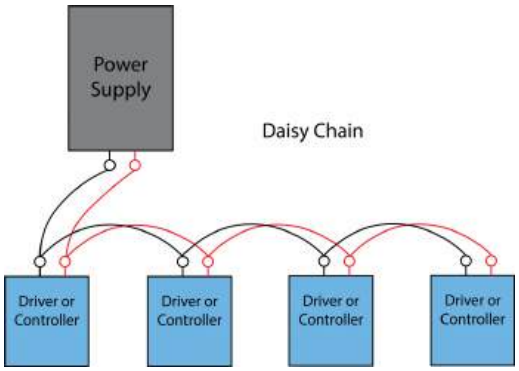


Figure 11: Daisy chain wiring diagram.

Furthermore, to address challenges associated with wiring complexity and system reconfiguration typical to CAN systems, a daisy chain topology was implemented. This strategy involves connecting multiple system nodes in sequence, akin to linking flowers together to form chains or rings. By employing a daisy-chain approach, each system node features dedicated CAN and power inputs and outputs, simplifying system expansion and reconfiguration while minimising wiring complexity and length. By adopting a modular architecture, the telemetry system offers excellent expandability, enabling seamless integration of additional sensors and functionalities to meet evolving project and user needs. Further strengthening the team's adherence to FOCs 6.1.0 and 6.2.0.

**Robust:** During the testing phase, a significant obstacle was encountered related to hand-soldered prototype boards, leading to inconsistent results. This was due to loose connections between wires and solder joints. These unreliable connections often broke, necessitating makeshift repairs and compromising the system's reliability. Identifying faults became challenging as they could stem from various sources.

To overcome these reliability issues and ensure consistent performance, the need for a method that offers repeatability, precision, and cleanliness in circuit design, manufacturing, and assembly was required. Printed circuit boards (PCBs) emerged as the solution to address these challenges effectively. By transitioning to PCBs, repeatability, precision, and resource efficiency were achieved and enhanced, while also reducing the system's footprint. The inherent precision of PCB fabrication minimises the risk of loose connections and soldering defects, thereby improving the overall reliability of the system and meeting FOC 6.3.0.

**PCB development - Node computer:** The development of the node board circuit (i.e. "node computer") underwent several iterative stages to achieve an optimal design. The team prioritised creating a solution that was easy to assemble, intuitive, and clear. The initial iteration was crafted at the UCL Department of Electrical and Electronics Engineering (EEE) Lab in Malet Place, representing the culmination of early design efforts (Fig. 12).

The second iteration focused on maintaining functionality while reducing the overall size of the circuit. Introducing a daisy-chained cable mechanism, different form factors were experimented with to enhance assembly and accessibility. However, limitations in manufacturing capabilities at the UCL lab prompted a transition to external PCB manufacturing services.

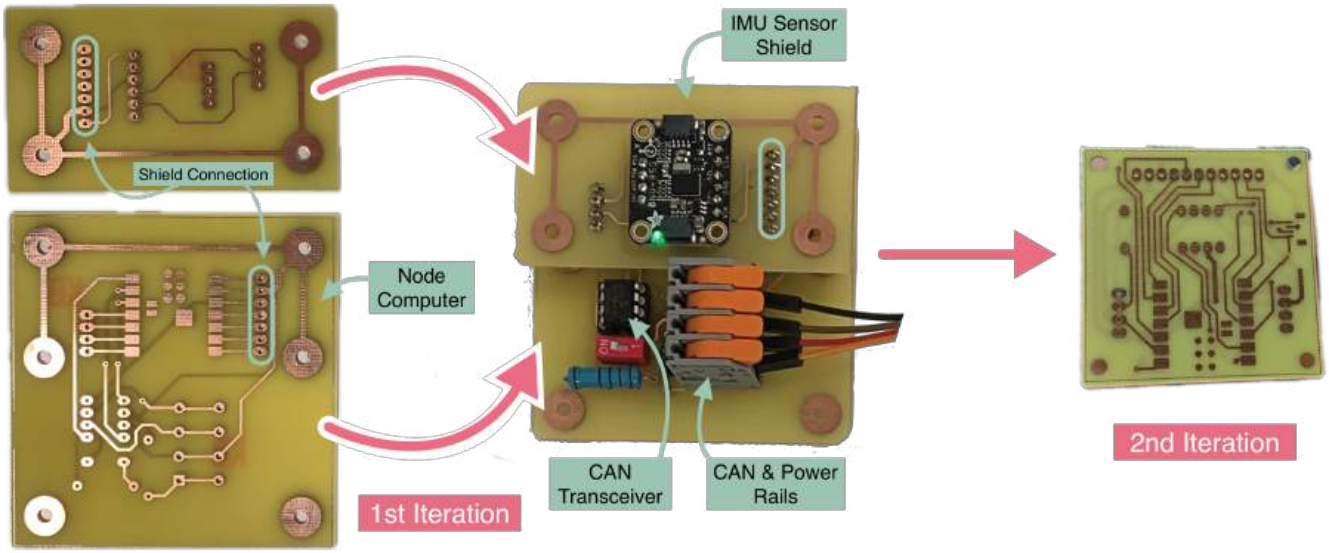


Figure 12: First and second node computer iterations, showing the attachment of a sensor shield onto the processing board.

The third iteration marked a significant advancement, as it was outsourced to a professional PCB manufacturing company (JLCPCB). This decision enabled faster miniaturisation. With the third iteration, the final footprint of the node computer was introduced. The selection of this footprint was driven by practical considerations, balancing the constraints imposed by the ESP32 development board's size with the requirements of the daisy chain connectors. The resulting design achieved a compact form factor, ensuring ease of manipulation and interaction for end-users (Fig. 13).

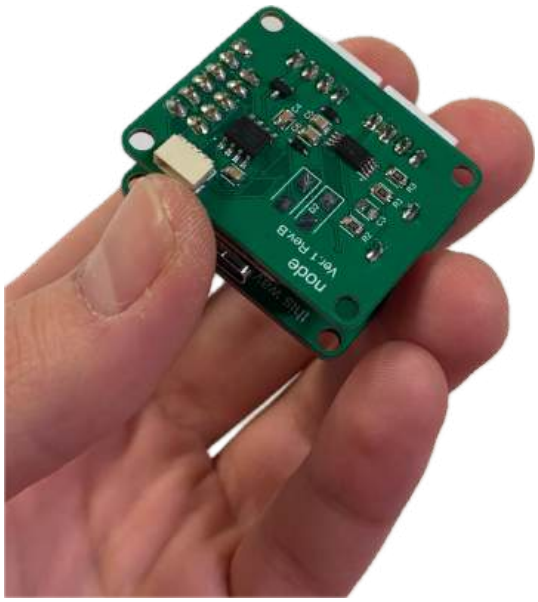

Figure 13: Underside of the third node computer iteration.

**PCB development - Receiver:** The system incorporates sensor nodes responsible for data acquisition, necessitating a complementary receiver board tasked with receiving, processing, storing, and managing radio communication concurrently. While the receiver board aligns with many of the requirements of the sensor nodes, its primary differentiator is its lack of need for expandability, as it does not directly interface with sensors.

The work on the receiver board commenced with the design of a spaced out development kit, featuring essential components such as a microSD socket, a 433 MHz radio module with an antenna connector, a CAN transceiver, and daisy chain JST connectors, interfacing with an ESP32-S3 microcontroller chip (Fig. 14).

Although the initial design exceeded spatial constraints, its larger form factor facilitated extensive troubleshooting and iterative refinement to address emerging issues effectively. This process informed the redesign, resulting in a smaller footprint with optimised pin connections and layout. The focus of the redesign was on the strategic placement of interactive components, such as switches, connections, and the SD socket, for the second and final iteration. Additionally, the initial iteration provided a platform for initiating the system's software development, marking a crucial milestone in the project's progression.

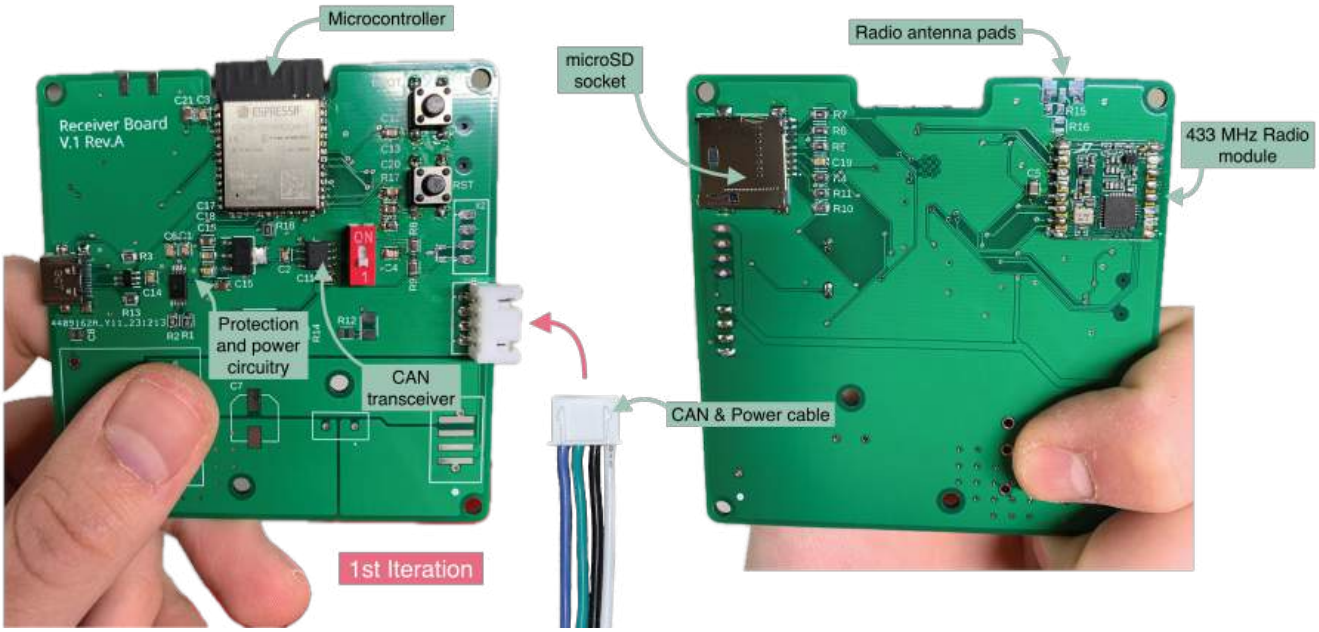


Figure 14: Top (left) and bottom (right) sides of the 1st receiver board iteration.

**PCB development - Ground station:** The ground station serves as a vital component of the project, acting as the interface between the race engineer and the vehicle's onboard systems. Its primary function involves receiving radio-transmitted data from the vehicle's receiver board, processing it, and transmitting it via USB to a laptop for display and analysis.

Given its role as a remote monitoring device, the ground station's design priorities differed from those of other circuits in the project. While resource efficiency and expandability were not paramount concerns, the team remained committed to optimising the design for cost-effectiveness, robustness, and user-friendliness.

With a simplified architecture comprising only essential components (a microcontroller, a radio module, and an antenna connection) the ground station naturally had a compact footprint. This compactness facilitated versatile deployment options, allowing the device to be mounted discreetly on the back of a laptop, tucked into a pocket, or integrated into larger antenna structures as needed.

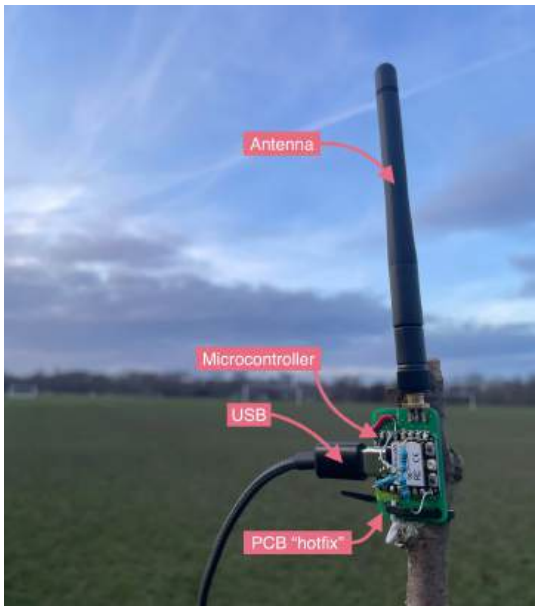


Figure 15: Ground station being tested in Regent's park (London, UK).

Despite its simplicity, the ground station's design underwent rigorous testing and refinement to ensure optimal performance and reliability.

**PCB development - Testing & debugging:** The journey from conceptualising an electrical circuit to achieving a fully functional PCB is rarely a smooth one. Despite meticulous planning and design, the reality of electronics development often presents challenges that demand rigorous testing and debugging efforts. This phase is crucial, as it bridges the gap between theoretical design and practical implementation.

A significant portion of the development timeline was dedicated to identifying and rectifying issues within the circuitry. Each iteration of the PCB underwent thorough testing to uncover potential faults or malfunctions. For instance, during the initial stages, connectivity issues were encountered between components due to improper soldering or faulty traces. These issues were identified through systematic testing methodologies such as continuity checks and signal tracing.

Furthermore, as the complexity of the circuit increased with successive iterations, so did the likelihood of encountering compatibility issues between components. For example, in one instance, we observed erratic behaviour in the node computer's sensor interface due to impedance mismatches between the sensor module and the microcontroller. This necessitated meticulous analysis of datasheets and voltage levels to pinpoint the source of the discrepancy.

Throughout the testing and debugging process, an iterative approach was adopted, wherein each identified issue prompted iterative refinements to the PCB design. This iterative feedback loop not only facilitated incremental improvements but also served as a valuable learning experience, informing future design decisions and best practices.

Figure 16: Jumper wires soldered onto the ground station PCB for debugging.

### 4.1.4 Final Solution

In the Deliver stage, the comprehensive electronic system was finalised, prepared for evaluation, and subsequent refinement. This systematic approach ensured a thorough exploration of design options while prioritising end-user requirements and meeting the FOCs throughout the development process.

**Nodes:** The final node computer design (Fig. 17) incorporates two JST daisy-chained CAN and power connectors labelled 'CAN In / Out', a female pin header for connection to the sensor shield's microcontroller digital pins (shown in Fig. 18), and a standard sensor manufacturer connector (Qwiic / Stemma QT). Additionally, the design includes essential protective circuitry such as a transient-voltage-suppression (TVS) diode to safeguard CAN lines from overvoltages, a low voltage drop Schottky diode to enforce one-way current flow, and capacitors to mitigate power surges. Each node features a switch to activate its CAN termination resistor, facilitating CAN bus extension with termination at each end.

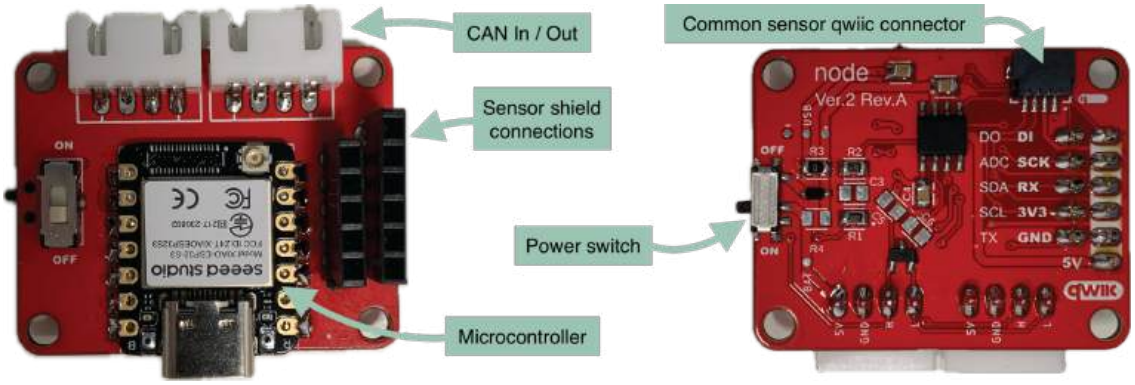


Figure 17: Close-up of the final node computer.

This design fulfils all specified requirements. It offers easy expandability (FOC 6.2.0), facilitated by the daisy-chained CAN configuration, and requiring only the design of a sensor shield (Fig. 19). It ensures robustness by utilising a resilient communication protocol, with optional footprints for improved reliability through the addition of capacitors and resistors (FOC 6.8.0). The design also provides user-friendly flexibility in connecting to sensors,

CAN, and power through the incorporation of switches and common connectors (FOC 6.1.0). Moreover, it features low power consumption from using few components (FOC 6.6.0), a compact form factor (FOC 6.5.0), and relatively low cost, with component expenses totalling approximately £10 per node computer (FOC 6.7.0).

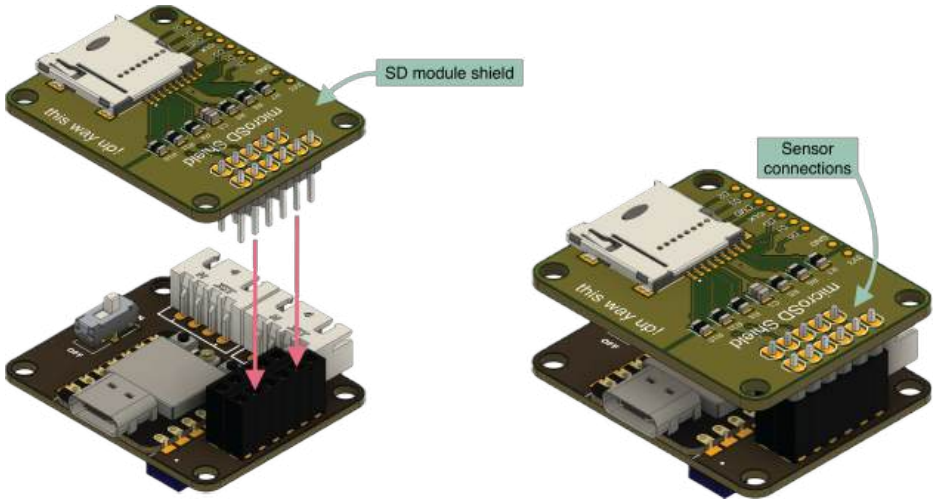


Figure 18: Diagram of the attachment mechanism of a sensor shield onto a node computer.

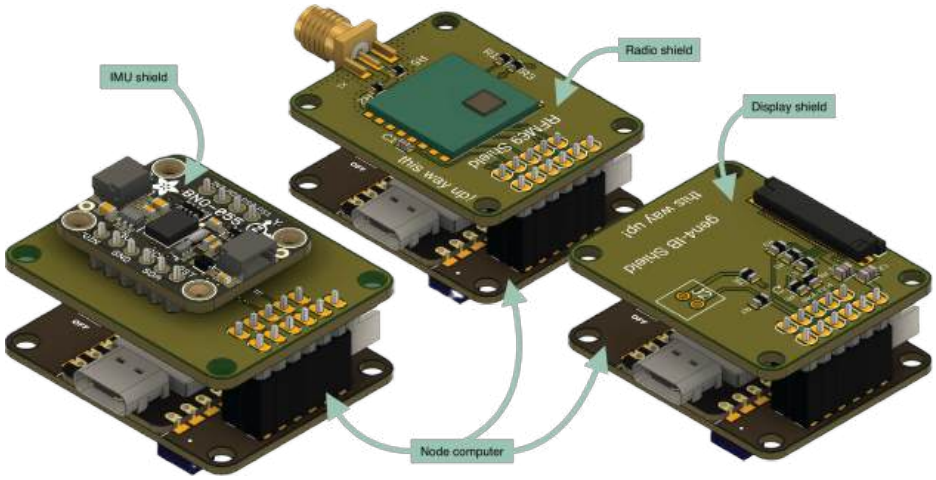


Figure 19: Examples of possible shield combination forming the nodes.

**Receiver:** The final receiver design (Fig. 20) integrates essential components for seamless operation within the system (FOC 6.1.0). It includes CAN and power connectors to distribute power to the entire system, along with a separate power-in connector from the power source for a safe separation. Additionally, the receiver features a microSD socket (FOCs 4.0) and a radio module (FOC 2.2.0), with an increase in radio signal performance. It has a mode switch button, which can be programmed to select different options while powered on. This will enable the development of different telemetry system configurations, giving the user more flexibility (FOCs 6.1.0 and 6.2.0). Similar to the node computer, it incorporates protection circuitry and electro-static-discharge protection on the USB connection.

This design meets all specified requirements (FOCs 1.0, 2.2.0, 4.0, 6.0). It ensures robustness through the incorporation of necessary protection measures and separation of power sources for added safety. Furthermore, the receiver's compact form factor, low power consumption, and cost-effective design totalling to around £25 per board, contribute to its overall efficiency and reliability.

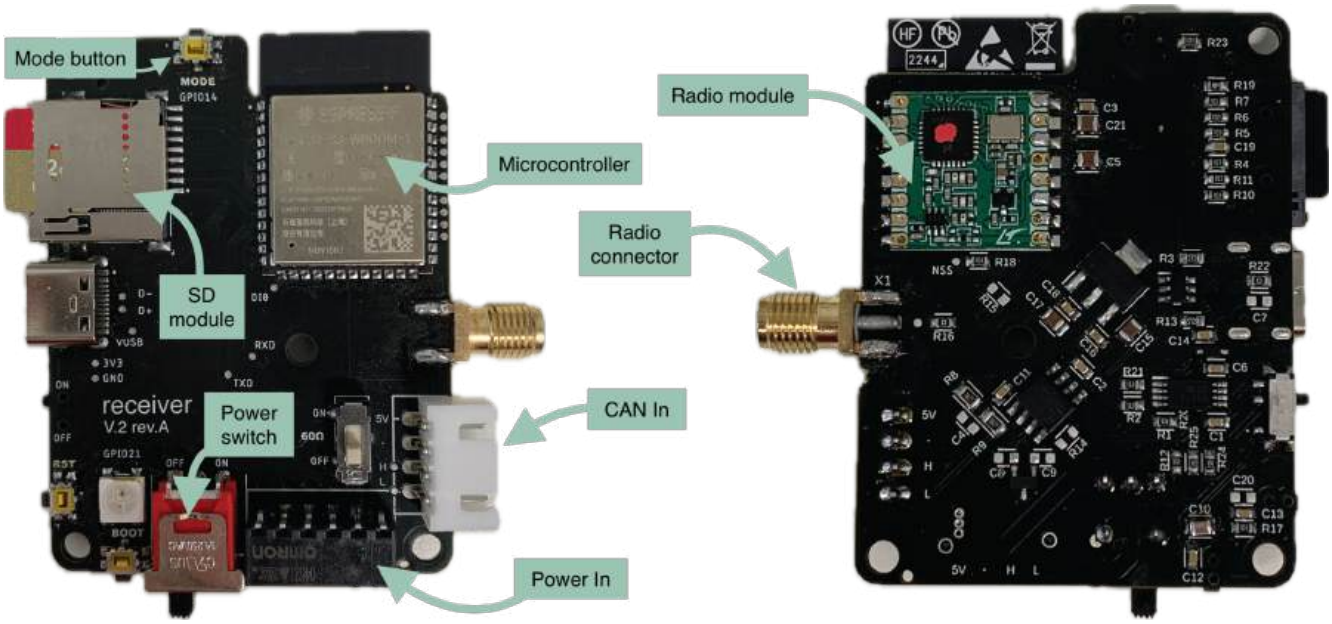


Figure 20: Close-up of the final receiver board.

**Ground station:** The final ground station design (Fig. 21) maintains its original form factor, now enhanced with pull-up resistors to address specific needs when utilising the radio module with the ESP32-C3 microcontroller.

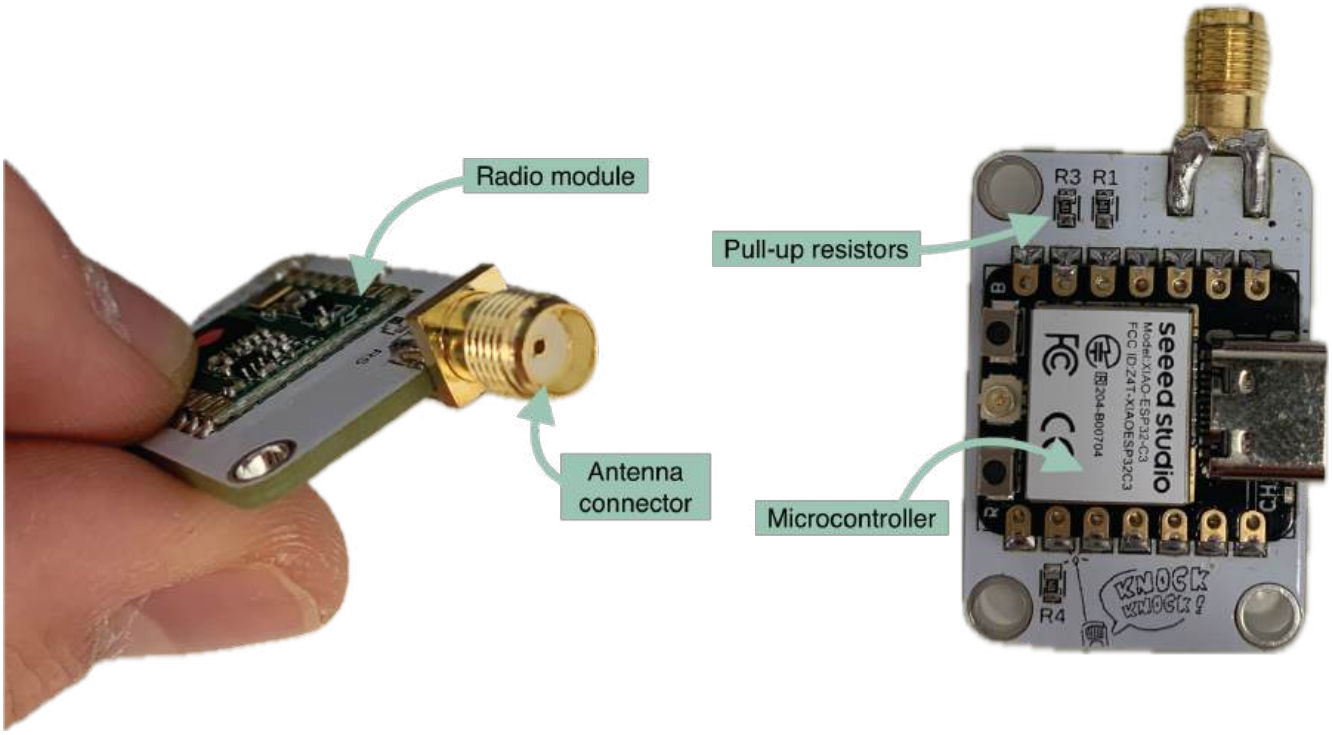


Figure 21: Close-up of the final ground station.

This design aligns with all specified criteria by its compact size (FOC 6.5.0), minimal power usage (FOC 6.6.0), and cost-efficient assembly, totalling approximately £10 per board (FOC 6.7.0).

## 4.2 System Information Design

In parallel with the development of the circuits, the behaviour of the system was continuously developed. It focuses on designing the interactions within the network to achieve data gathering (FOC 1.0), communication (FOC 2.0), processing (FOC 3.0), storage (FOC 4.0), and visualisation (FOC 5.0). The main goal was to develop a simple, scalable solution that can be implemented in future UCL Shell Eco-marathon projects without the team's presence.

In the Discover and Define phases, the functions of each component along with the architecture of the system are defined. Then in the Develop and Deliver phases, methods capable of achieving the desired functionality are outlined, and a final design is presented.

### 4.2.1 Discover

As described in the previous section, the overall system consists of an arbitrary number of nodes, a receiver and a ground station. This section defines the function each component plays in the overall system.

- **Nodes:** Nodes were designed for two tasks: taking measurements, and communicating it over CAN. The amount of nodes in a system depends on the use case, necessitating the system to be easily scalable.
- **Screen node:** The screen node is a unique node, because instead of putting readings on to the CAN bus, it instead continuously reads them, communicating relevant data to the driver.
- **Receiver:** The receiver processes data coming through the CAN bus, storing it and/or sending it wirelessly to the race engineer.
- **Ground station:** The ground station receives the wirelessly transmitted data and sends it to the race engineer's computer, where it is further processed and displayed.

### 4.2.2 Define

With these functions in mind the architecture of the system can be designed. Information flows internally through the CAN bus from the nodes to the receiver, with the screen node tapping into the network. The receiver then stores the information internally, and transmits it to the ground station, where it is displayed to the race engineer (Fig. 22).

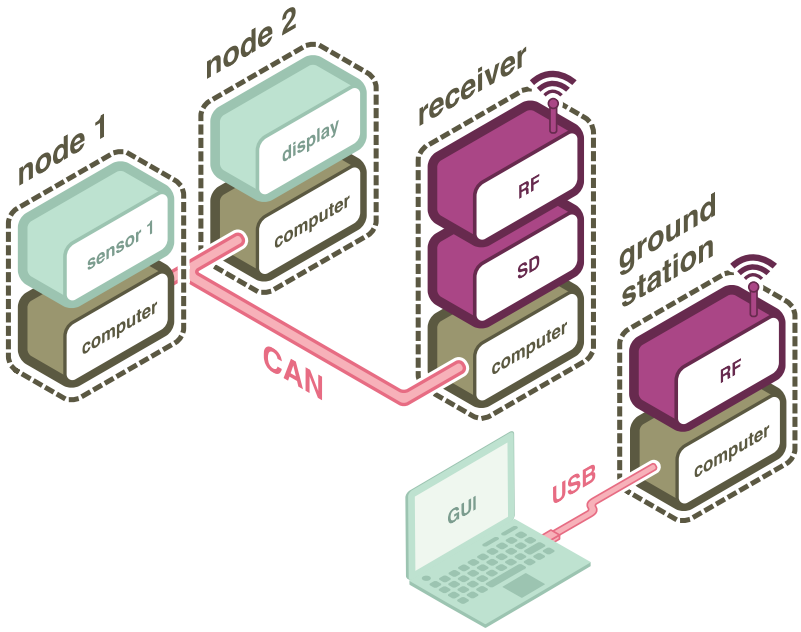


Figure 22: The architecture of the telemetry system.

### 4.2.3 Develop

The components in the system are categorised based on their functionality. Data gathering is done by the nodes. Data processing is done by the screen node, receiver, and the ground station. The ground station and screen also perform data visualisation. Apart from this, there is also communication between the components via wired or wireless methods.

**Data collection:** As described in the electrical design section, the system requires the measurement of position, forces/acceleration, voltage, and current, which is done via sensors. Hence, requiring a node for each of these quantities, resulting in a total of seven nodes. Four voltages need to be measured, three relating to the engine and one to the throttle. A voltage node can measure two voltages, hence the need for two voltage nodes. These measurements are communicated via CAN to the receiver and screen node.

**Data processing:** CAN messages from the nodes are sent to the receiver and the screen node. The receiver decodes and stores them (FOCs 3.1.0, 3.3.0, and 4.1.0). No further computation with the sensor readings is done by the receiver. Whereas on the screen node data is not being stored, the raw readings are continuously being processed to display relevant processed data to the driver via a screen (FOCs 2.1.0, 2.3.0, 3.1.0, and 3.2.0). The processing and visualisation is discussed in detail in section 4.3.

The receiver sends raw sensor readings via RF messages to the ground station for real-time data analysis of the driver's performance (FOCs 2.2.0, 2.3.0, 3.2.0, and 3.3.0). This is done by producing plots that can be interpreted quickly and acted upon so that the driver's performance can be improved during the race (FOC 5.2.0). Section 4.3.2 describes the race engineer interface in more detail.

**Wired communication:** The CAN bus serves as the cornerstone of the system; its failure would lead to system-wide breakdown. Thus, enhancing the robustness of its implementation became imperative, necessitating improvements in circuit design as seen in section 4.1.3. However, theoretical enhancements alone lack the capacity to validate their efficacy. Therefore, a comprehensive testing framework was essential to gauge the impact of these modifications.

To this end, a rigorous testing methodology was adapted inspired by the examination outlined in the Texas Instruments Application Report on CAN Transceivers [25]. This methodology involves subjecting a two-node CAN network (nodes A and B) to a range of experimental conditions, detailed in section 4.1.1, to evaluate its performance and identify areas for potential improvement.

Central to the evaluation of the two-node CAN network is the transmission of a million messages between node A and node B, and vice versa, or until one node fails and enters a bus-off state. Throughout these tests, the error registers of the nodes are meticulously monitored to assess the transceiver's performance and the operational status of the network. Instances of excessive errors serve as indicators of experimental conditions unsuitable for practical application.

This testing methodology has played a crucial role in advancing the development of the system. By facilitating thorough debugging and pinpointing the root causes of failures, it has paved the way for the refinement of the implementation, as discussed in detail in Section 4.1.4.

**Wireless communication:** Wireless communication is necessary to transmit data on the driver's performance during the race to the race engineer. The team analysed the racetrack to identify the required signal range to send the data in real-time (FOC 2.2.1), independent of where the vehicle is on the track (Fig. 23). The antenna will be located in the stands. The stands are on a metal rooftop, blocking the transmission of radio signals on the two vertical sides of the box in the image. Assuming there is no blockage of the radio signals, the percentage of the track covered for each antenna range is shown in Table 8.

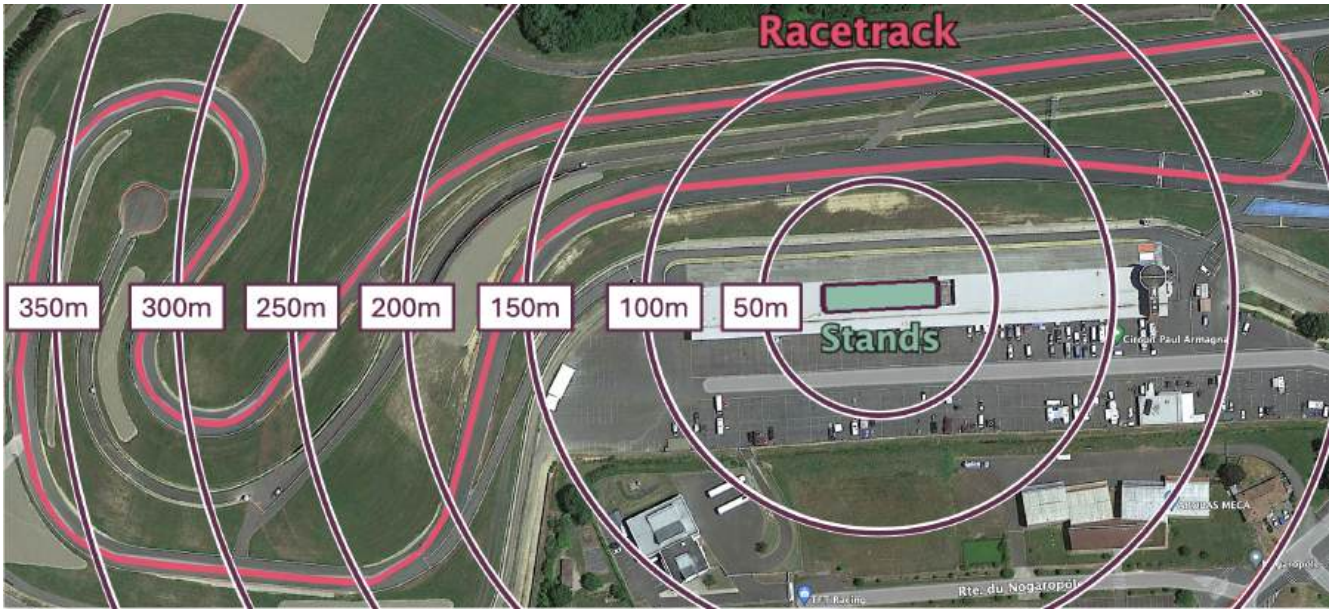


Figure 23: Track coverage as a function of antenna range.

Radio communication was the method chosen for wireless communication. FM Radio was selected for the reasons presented in section 4.1.2. The selected radio module has the limitation of only being able to send 58B of data per message. This means that 58 characters can be sent in a message. Table 9 shows how many characters/bytes each measurement takes up. The table does not take into account the fact that each measurement requires a unique ID to identify it. This analysis led the team to consider various sending methods to reduce the message length.

Table 8: Nogaro track coverage as a function of antenna range.

| Range (m) | Track coverage (%) |
|---|---|
| 50 | 0 |
| 100 | 16.2 |
| 150 | 34.1 |
| 200 | 53.7 |
| 250 | 63.3 |
| 300 | 76.1 |
| 350 | 88.3 |
| 400 | 100 |

Table 9: Sensors in the vehicle along with the length of each parameter being measured.

| Sensor | Quantity | Characters |
|---|---|---|
| **IMU** | x acceleration | 5 |
| | y acceleration | 5 |
| | z acceleration | 5 |
| **GPS** | Latitude | 8 |
| | Longitude | 8 |
| | Time | 10 |
| **BMS** | Voltage | 3 |
| | Current | 3 |
| | Power | 3 |
| | Coulomb | 3 |
| | Temperature | 5 |
| **Throttle** | Position | 3 |

Assuming that the team will utilise the maximum message length, a model was constructed to identify the minimum radio range that is required to ensure that measurements do not stockpile without being sent. This was done by using data from last year's competition to get an estimate of how long it takes to complete a lap. Combining this with the sampling rate of each sensor, the amount of data gathered each lap can be estimated (Fig. 24). It was determined that the minimum sending range is 200m to prevent data accumulation. While a range of 250m would ensure that the data is sent within the same lap it was gathered in. Having a 400m range would enable continuous data transmission. Any range above 400m is redundant and would consume more energy, negatively impacting the team's performance. These design choices were evaluated via testing, detailed in section 5.2.1. It was concluded that sending live continuous data throughout the race is not necessary. Because, improvements can only be applied in subsequent laps after the measurements are taken. Hence, FOC 2.2.0 and FOC 2.3.0 will not be met. To optimise sending efficiency, only relevant measurements will be sent, reducing the data size. Hence, messages will be sent in batches.

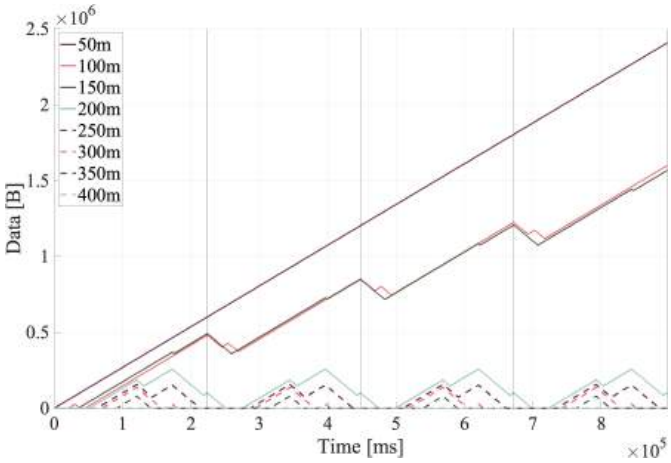


Figure 24: Data profile of a lap with various ranges.

**Storage** The receiver is responsible for storing the data gathered throughout the race. Data is stored via an SD card. The stored data is classified depending on whether it is sent wirelessly or not. Such operations of quickly writing and reading from an SD card can result in corruption of the file. That is why the data to be sent is stored in a separate directory on the SD card. In case it does get corrupted, it only compromises the team's wireless communication and not its data gathering, allowing for post race analysis. Every reading is stored on the SD card regardless whether it is being sent or not. Each sensor has its own file to which its readings are stored, along with its timestamp.

Since the sensors in the network have different sampling frequencies, and can sometimes go offline during the race, storing them separately allows for the identification of when a new measurement has been taken and also whether the sensor is taking measurements. This file structure meets the requirements defined by FOC 4.2.0. The data to be sent is stored in a separate directory. As mentioned in the wireless communication part data will be sent in batches. Once, the vehicle is in sending range, it will start sending data from this file, each message transfer has an acknowledgement associated with it, to identify whether a message transfer was successful or not. If unsuccessful the message will be resent, satisfying FOC 2.4.0.

### 4.2.4 Deliver

Figure 25 shows the final design and the flow of information throughout the system. The four goals of gathering, processing, storing and displaying data are done by various nodes in the system. Data flows in one direction from the nodes (data source), to a storage or visualisation method (data sink).

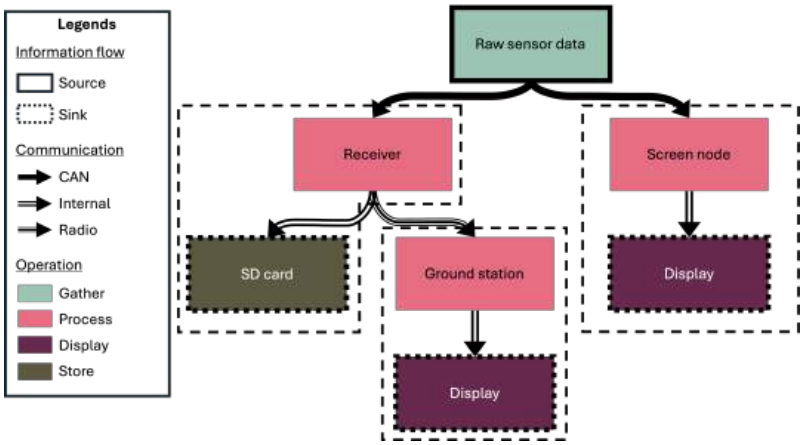


Figure 25: The flow of information throughout the system.

## 4.3 Data Visualisation and Processing

### 4.3.1 Live Driver Interface

At the competition, the driver's performance is judged by their ability to finish the 10-lap race in under 38 minutes while minimising the vehicle's total energy consumption. To achieve optimal performance, the driver needs feedback on how their driving style impacts lap times and the vehicle's energy consumption. The live driver interface is the subsystem responsible for conveying this information to the driver.

**Discover and define:** The Discover phase involved understanding the driver's needs through a series of interviews, combined with the initial literature review. Close collaboration with the user ensured that the final product

is specifically tailored to their needs and preferences (FOC 5.2.1). Once understood, the user's needs are translated into feature requirements. These features define the information that must be communicated to the user via the driver interface. In Table 10, features listed first were assigned higher importance by the driver.

Table 10: Information features communicated by the interface.

| **Category** | **Feature** | **Explanation** |
|---|---|---|
| **Progress Indicator** | Lap Counter | Represents the current lap number |
| | Final Lap Alert | Alerts the driver when the final lap has begun |
| **Performance Indicator** | Target Lap Delta | Represents the difference between actual lap time and the target lap time, calculated from race simulations |
| | Race Time | Represents the time remaining to end the race within the 38 minutes limit |
| | Best Lap Alert | Alerts the driver when a new most energy efficient lap is completed. This is calculated each time the start-finish line is crossed |
| | Continuous Energy Delta | Given the vehicle's current position on track, this is calculated by comparing the total energy consumed up to that point in the current lap with the total energy consumed at the same point during the best lap |
| | Continuous Time Delta | This is calculated by comparing the current lap time with the lap time for the same point on track during the best lap |
| | Sector Energy Delta | As the vehicle completes a sector, this represents the difference between energy used during the sector and energy consumption over the same sector during the best lap |
| | Sector Time Delta | This represents the difference between the time taken to complete the sector and the time taken to complete the same sector during the best lap |

There are two types of features required by the driver: race progress and performance indicators. Race progress indicators describe the driver's overall progress through the 10 laps of the race. While performance indicators compare current performance to the best (i.e. most energy efficient) lap recorded during the entire race. Each performance indicator has an energy and time component as it is crucial to use both energy consumed and time elapsed to make driving decisions, given the competition's focus on achieving the highest energy efficiency while remaining within the time limit.

Once the interface features are defined, the method of communication can be investigated. In the automotive sector, information is communicated to the driver primarily through visual, auditory and tactile mediums. Criteria to evaluate different communication methods were identified using driver interviews. As with the information features presented previously, these encapsulate the driver's individual preferences.

Table 11: Metrics to evaluate interface technologies.

| **Rank** | **Evaluation Metric** | **Explanation** |
|---|---|---|
| 1 | Information Clarity | Information is presented simply and can be interpreted quickly |
| 2 | Information Reliability | Information presented is consistently available and correct |
| 3 | Uninstrusive to Vehicle Operation | The interface doesn't obstruct the driver's view through the front or side windows or interfere with the driver's ability to operate the vehicle |
| 4 | Uninstrusive to Vehicle Evacuation | The driver can exit the vehicle within ten seconds, when the interface is installed, as stated in the competition regulations [26] |

Ultimately, a visual communication method was chosen. This is the least intrusive to the driver's ability to operate the vehicle and information can be packed more densely compared to auditory and tactile methods. Various display

automotive technologies such as analogue dials, heads up displays and segment display were evaluated using the criteria in the table above. Amongst these, an LCD screen was chosen because of its potential for high information density (FOC 5.1.1), customisability through programming and availability in various sizes. Within the vehicle, the display module is fixed to the back wall on the left-hand side of the driver's seated position so that it does not hinder their ability to evacuate the vehicle. Safe evacuation is required by Article 30a of the competition regulations and helps meet FOC 5.2.2 [26].

**Develop and deliver:** Once the display technology was specified, the display module's size was determined through in-situ user testing. In the seated driving position, the driver's eyes are 80cm away from the screen. At this distance, it was determined that the smallest font size viewable with acceptable clarity has a character width of 0.9cm and height of 1.3cm. Using this optimal font size for all the features mentioned in Table 10 specified a display with a minimum active area of 150mm (width) by 80mm (height). The gen4-uLCD-70D display module by 4dSystems was selected based on this requirement. This module's display is driven by a dedicated microprocessor and storage, which allow it to be configured as a serial peripheral device commanded by the node microcontroller. This configuration drastically frees up computational resources on the host microcontroller for data processing and CAN communication tasks. Optimising processing speed helps achieve FOC 5.1.2.

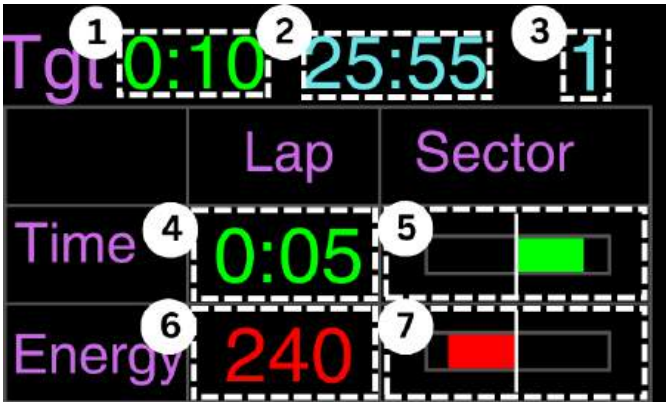

Figure 26: Initial driver interface.

**Initial interface:** Figure 26 shows the initial interface that was designed and programmed onto the display module. The highlighted elements represent the following data:

- 1, 2 and 3: Target lap delta, race time, and lap counter respectively.
- 4: Lap time delta in 'm:ss' format.
- 5: Lap energy delta in kJ.
- 6 and 7: Sector time and energy deltas. Positive deltas (green) and negative (red). The length of the bar is proportional to the magnitude of the delta.

In line with the team's focus on rapid prototyping and practical design evaluation, the interface was tested in-situ by the driver. The results of this testing, summarised in Table 12, highlighted areas for improvement concerning the colour scheme, text and layout of graphical elements. It also exposed the technical constraint of the graphical library's lack of support for drawing animated objects.

Table 12: Driver feedback on the initial interface design.

| Design Category | User Feedback | Solution |
|---|---|---|
| **Colour Pallet** | Green and orange were poorly visible when the display was viewed at an an off-angle | Use alternative high contrast colours |
| **Use of Text** | 'Timer' and 'Energy' text labels were unnecessary and restricted space available for the information elements | Remove text or replace with icons |
| **Layout** | Grouping elements into a table distracted from the information elements | Remove the separation grid and increase the size sector delta elements |

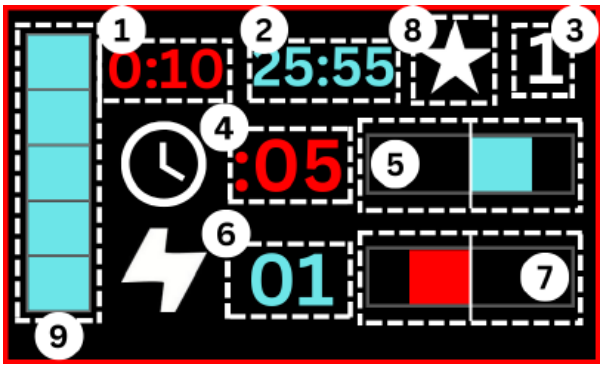

Figure 27: Final driver interface.

**Final interface:** The final interface was designed by incorporating the user feedback (Fig. 27). The additional elements are:

- 8: Best lap icon which flashes when a new best lap is achieved to provide more context to the deltas.
- 9: Super capacitor State of Charge (SOC), from which the supercapacitor health is inferred.

All other elements are the same as previously. From the Eco Marathon team's previous experience with using digital displays in the vehicle, a display with 800lux of brightness is visible to the driver during the competition. However, the uLCD-70D display module has a maximum luminance of 500lux. Therefore, even at maximum luminance, the display would be difficult to view.

**Visibility mitigation:** Mitigation strategies were required to reduce the luminous intensity inside the vehicle. In the automotive industry this is accomplished through tinting. Tinting is the process of covering a transparent surface such as windows or headlights to limit the amount of transmitted solar (primarily visible and infrared) radiation. However, the vehicle's polycarbonate windows are unsuitable for conventional automotive tints due to the steady-state release of gases trapped within the polymer known as outgassing [27]. Outgassing can reduce the optical clarity of the windows over time. However, vinyl films allow gasses to diffuse from the material surface, protecting the window's optical clarity.


Figure 28: Vehicle side windows with (above) and without (below) the vinyl films attached.

With the vinyl film material selected, the appropriate VLT (Visible Light Transmission) value was determined by simulating the ambient luminosity at the Nogaro circuit using high-powered spotlights. Films of various VLT values were fixed to the side windows and the value sufficient to make the display visible at maximum brightness was recorded. With the competition regulations in mind, a film with a 50% VLT was fixed to the vehicle's side windows. Although the display has been tested to be comfortably viewed in the local conditions at Nogaro, at maximum brightness, doing so it consumes 750mA of current. This power consumption is significant compared to the other components in the Telemetry system, as discussed in Section 5.3.1.

To mitigate this, a two state toggle switch was installed to turn the display on and off. It is located in the controller stick the driver uses to steer the vehicle, making it easy to access. The driver can use this to turn the display on during sections of a lap, primarily when leaving corners. After reviewing their performance, the display can be switched off. Assuming the driver uses the screen for five seconds after each of the seven corners at Nogaro, the display's energy consumption decreases by 83%.

### 4.3.2 Live Race Engineer Interface

The live race engineer interface collects wireless data from the antenna mounted on the car, allowing the race engineer to evaluate the driver's performance in real time, and enabling them to offer feedback to improve the car's efficiency by identifying patterns in the data (section 4.3.3).

**Discover and define:** The background of the race engineer interface was created by extensively studying the books mentioned in the literature review [5, 13], along with the input from the race engineer. It was decided that the race engineer interface should be able to show the most relevant information of the vehicle, which in this case are its velocity, current and voltage at various points in the engine (FOC 5.2.1).

**Develop and deliver:** A Matlab application was developed that is capable of meeting these requirements (Fig. 29). It has four main sections. Section 1 allows for the connection of the Ground Station to the computer, and it also

displays the current lap along with a timer. Section 2 has the toggle switches which allow for the selection of which data is plotted on the graphs (FOC 5.1.0). Section 3 is the velocity plot, showing the vehicle's velocity throughout a lap. The lap toggle allows for the selection of which lap's data is plotted. Section 4 has plots that compare voltages and currents at various points within the car and on various laps. These three plots give information to the race engineer about the driver's performance along with the state of the vehicle. A contingency plan is also in place in the case that the application fails, a VS Code library called Teleplot will be used instead [28]. Teleplot can instantly plot data coming through the serial, however it does not have a straightforward way to implement the toggle functionality that allows for the overlay of data, making its plots less useful. To ensure that the data sent by the Ground Station is compatible with both the Matlab application and Teleplot, the Matlab application uses Teleplot's data format.

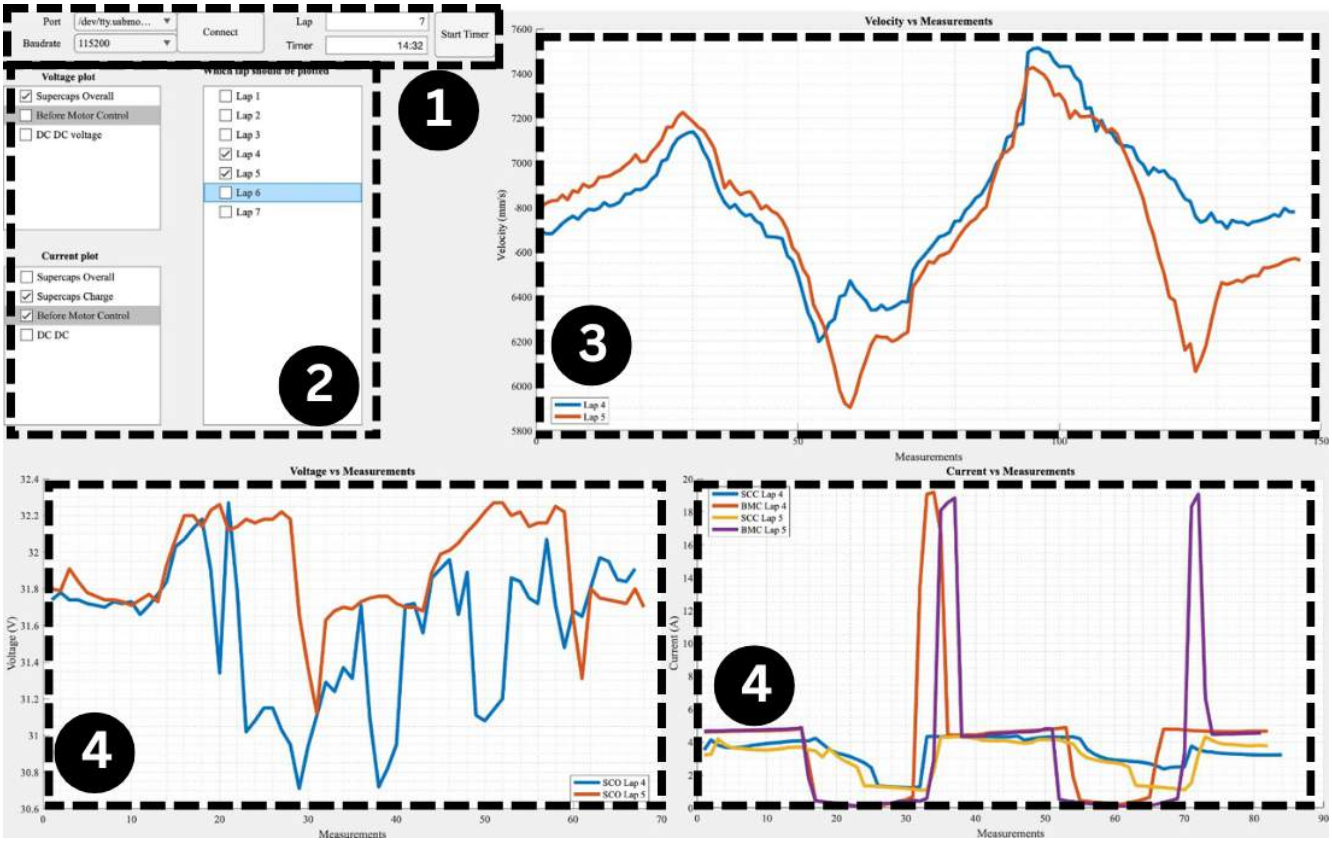


Figure 29: Final race engineer interface showing test data from Cyclopark.

### 4.3.3 Data Analysis

The telemetry system is impractical without a means of evaluating and analysing the data. Mark Twain put it more frankly: "Data is like garbage. You'd better know what you are going to do with it before you collect it". This not only highlights the famous novelist's engineering inclination, but also the need to identify the performance indicators derived from the raw data that improve the car's efficiency. The live driver and race engineer interface predominantly use raw sensor data. However, more computation heavy algorithms can be developed to process this information post-race. This would enhance the team's understanding of the car's behaviour on track and how it influences the energy losses. This can be done through both race strategy and technical innovation. The aim of the data analysis is not only to highlight driving patterns that will minimise the power consumption at the competition, but also areas of improvement in the chassis to reduce energy losses.

**Discover and define:** The performance at Shell Eco-Marathon is ranked solely on the fuel consumption for the marathon race. Until the hydrogen system was ready for on-track testing, the car ran on batteries. Therefore, the telemetry system must be capable of measuring both hydrogen flow and electrical energy usage to evaluate the car's efficiency. This is closely linked with the driver's power deployment and handling around the track. The car's movement and velocity trends should be identified to observe which race lines minimise the energy losses.

Moreover, these also determine the resistive forces acting on the car. The data should be arranged and presented on a lap-by-lap basis. This would allow for tracking of the driver's evolution and comparison of the car's behaviour and related performance indicators. This insight should be displayed and presented to the driver to aid his preparation for the competition, and allow the team to evaluate what car inefficiencies can be addressed to develop a better chassis.

**Develop and deliver:** To develop all of these functionalities, the team has created a MATLAB algorithm which will be used to evaluate the car's performance. The software was designed to require minimal input from the user (FOC 5.2.0). Once the data folder is loaded from the SD Card, the software displays an overview of the entire racing session in terms of total distance travelled, energy consumption, efficiency rating and average velocity. Then the lap is sorted lap-by-lap to identify the most efficient run on-track. The following step is for the user to input the lap number of the two laps that will be compared to identify racing patterns that optimise the racing strategy. The MATLAB algorithm outputs are presented in the Results section of the report, using data from testing the on UCL's Shell Eco-Marathon car on track.

## 4.4 Casings

Casings were required to protect electrical components such as PCBs, sensors, antennas and the driver display, whilst ensuring that they do not interfere with the operation and functionality of each component. The iterative design process was adopted to ensure that the designs satisfy the requirements set out in the FOCs.

### 4.4.1 Microcontroller Casings

**Discover:** The design requirements of the nodes were specified. These focus on access to the ports, the mechanism for connecting the sensor shield to the node, and the location of the nodes within the vehicle. This results in an initial definition of the overall dimensions of the casings. Further research was conducted to understand existing designs of protective electrical casings. Based on this research, various prototypes were made to evaluate their suitability for this application.

**Define:** From the prototypes tested, certain FOCs within FOC 6.0 System Design were further elaborated upon to make it more specific for the casings. Table 13 shows the FOCs that were modified.

Table 13: FOCs 6.0 further elaborated for casings.

| Objective | Constraint |
|---|---|
| **6.1.0** Easy to use | **6.1.1** System can easily be taken apart and assembled multiple times |
| | **6.1.2** System can only be assembled in one orientation |
| **6.3.0** Easy to manufacture | **6.3.1** Manufacturing requirements and materials are easily available |

Figure 30: Initial IMU node computer casing.

Figure 31: Final IMU node computer casing.

**Develop:** With the newly elaborated FOCs, various designs were created and tested to identify whether they meet the design goals specified. The first design (Fig. 30) consisted of a 3D printed body holding the microcontroller and sensor, and a laser cut acrylic lid attached to it by bolts via heat inserts. Thus, a robust design was created that was easy to assemble and disassemble, meeting FOC 6.1.0. However, the overall size, weight, and installation of the heated inserts did not align with FOCs 6.5.0 and 6.3.0.

To mitigate these issues, the overall size of the casing was reduced to more conformally follow the shape of the PCBs, the infill density of the prints were reduced to make them lighter, and to simplify manufacturing, an innovative compliant mechanism was implemented to remove the need for nuts and bolts. This allowed the team to create casings that were entirely 3D printed, simplifying the manufacturing requirements to only a 3D printer, as opposed to the addition of a laser cutter and heating equipment for the heat inserts. This design change also made the design much more sustainable, by allowing failed prints or broken cases to be recycled and reused in printing new cases.

The team converged on a 3-piece design. The first piece, the base, securely holds the node computer in place, protecting its bottom. The second piece slots onto it via the compliant mechanism. This middle piece has cutouts on its sides to allow access to the ports of the node computer, while its insides act as a guide for attaching the sensor shield to the main controller. Finally, the third piece is a lid protecting the top of the sensor shield and attaches to the middle piece via the compliant mechanism. This 3-piece design went through several design changes from the original idea, as seen in Figure 33.

**Deliver:** With the design fully defined, the casing were finalised. First, the ideal compliant clipping mechanism was identified through testing. After testing numerous attaching mechanisms of different configurations, it was determined that the innovative spherical clipping mechanism stood out for its durability and reliability, by maintaining a firm hold even after repeated use (Fig. 32).

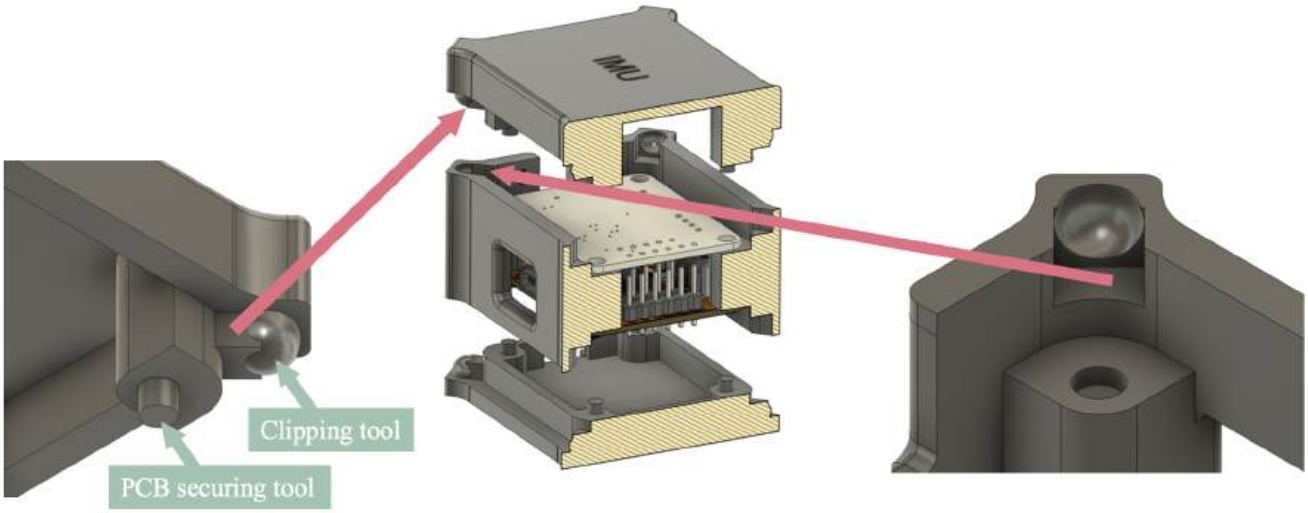


Figure 32: Final node case design and clipping mechanism.

Multiple iterations were conducted before finalising the design. Firstly, the thickness of the walls was reduced from 5mm to 3mm, which was achieved by moving the clipping mechanisms to the corners of the casing. The thinner walls enabled better access to the ports through a smaller gap between the ports of the PCB and the cutouts of the walls, enhancing usability. In addition, the initial design used long pillars that stem from the base and passes through the middle case to the top lid to secure the two PCBs. This proved to be fragile and prone to fracture. Therefore, the design was changed to incorporate two sets of shorter pillars, one attached from the base and the other attached from the lid. This helped to further improve the design's durability.

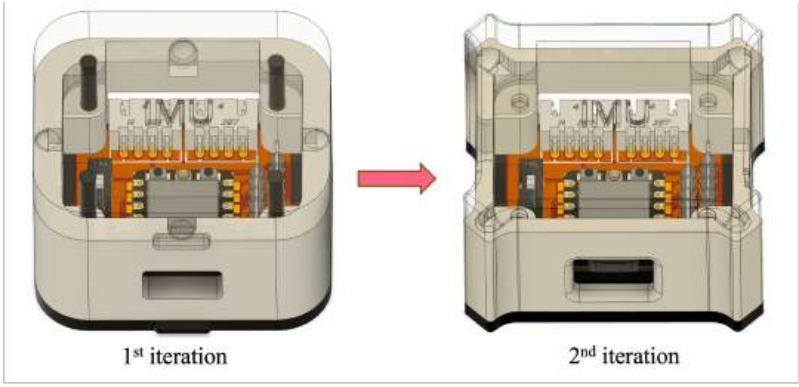


Figure 33: Data profile of a lap with various ranges.

Finally, due to the geometry of the design, the middle piece can be attached in two orientations to the base and the lid, with only one orientation allowing for the access of all the ports. To ensure that the user does not accidentally assemble the cases incorrectly, a slit was incorporated into one side of the casing. If assembled correctly, the slits align to form a straight line from the top of the case to the bottom, letting the user know that the casing has been assembled correctly. This approach also satisfies FOC 6.1.2. The final design shown in Figure 31 meets all the necessary FOCs.

The node computers' modular design allows the node to remain constant while the sensor board is interchangeable, depending on required function of each node. This enables the basic design features to remain the same and to be applicable to the GPS, screen, and power meter nodes. The various sensors, each with unique port access needs, are accommodated through adaptations in port opening locations of the case design. For example, the pluggable screw terminal of the power meter node shown by the green ports in Figure 34.

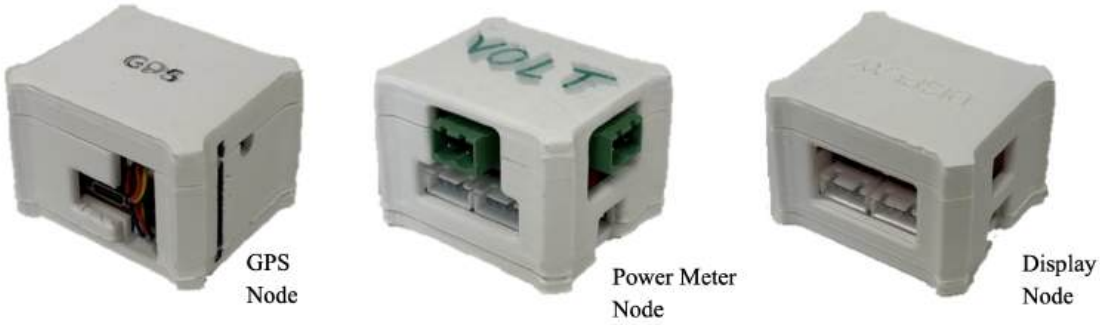


Figure 34: Variations of the design for different nodes.

### 4.4.2 Receiver and Ground Station Casings


Figure 35: Antennas casing.

Similar to the node computers, the double diamond iterative design process was used to continuously improve receiver and ground station casing designs to satisfy the FOCs. The final designs take inspirations from the node computer casings. The spherical clipping design was reused for its robustness and reliability despite differences in casing sizes. As the PCBs no longer needed to be stacked, the case consists of a two piece lid and base design. The final designs can be seen in Figure 35.

### 4.4.3 Antenna Casings

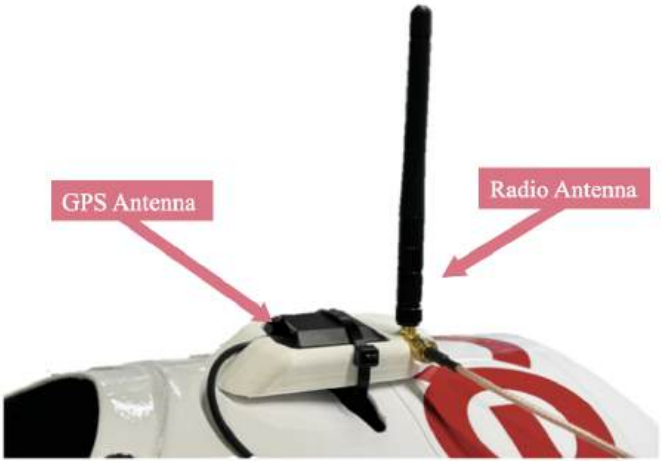


Figure 36: Antennas casing.

**Discover:** As the antenna from the GPS node and receiver need to be installed outside a vehicle, an antenna casing was developed to house the two antennas compactly.

**Define:** A primary requirement of the antenna system design is that it should be located at the tallest point of the vehicle so that the GPS and radio signals do not get obstructed. It also needs a clear view of the sky. Therefore, the top surface should be exposed. In addition, it needs to satisfy the constraint of having a small space available between the two movable covers of the vehicle. It also required good access to the holes that would enable access for the wire to reach the GPS and receiver nodes that are installed inside the vehicle. Lastly, it should have good aerodynamic performance.

**Develop:** Designs were physically tested, and computational simulations were conducted in later sections to ensure that the FOCs were met.

**Deliver:** The final design involves using an SMA (SubMiniature version A) extension cable to extend the radio antenna of the receiver to the vehicle exterior. It is then connected to a 90° SMA adaptor so that the radio antenna can be placed in the vertical direction without deforming the extension cable. The overall aim was to make the component as small and streamlined as possible to prevent interference with the vehicle's aerodynamic performance. The solution is shown in Figure 36. Its performance will be analysed in Section 5.1.

### 4.4.4 Driver Display

Figure 37: Driver's point of view.

**Discover:** The optimal tilt angle of the display screen and its ideal location within the vehicle were established through practical testing and interviews with the driver seated inside the vehicle, shown in Figure 37.

**Define:** By taking precise measurements during these sessions, its optimal angle and position were quantified as constraints. In addition, the driver mentioned that there could be glare from the sunlight entering from the side windows, hence, another objective was to shield the display from direct sunlight. The casing also requires access to the cable that connects the display to the screen node computer.

**Develop:** Different designs were experimented and consulted with the driver to ensure that the display was ergonomically positioned and securely mounted, with no obstructions to existing vehicle interior features to interfere with the driver's accessibility to vehicle controls. It also did not interfere with the drivers' ability to quickly enter and exit the vehicle, such that it satisfies the health and safety rules of the competition (FOC 5.2.2).

**Deliver:** Given the larger mass of the screen compared to other components, bolts and nuts were used to reinforce the stability of the assembly. This ensured that the screen remains securely in place even under dynamic conditions. Additionally, to enhance the screen's visibility in bright conditions, a visor was specifically engineered to shield the display from direct sunlight, shown in Figure 38. This feature is crucial for maintaining clear visibility and improving the driver's ability to monitor the system's outputs without interference from external light sources entering through the windows.


Figure 38: Display Casing Final Design.

# 5 Results

## 5.1 CFD

In this section, a Computational Fluid Dynamics (CFD) analysis was conducted to investigate the effect of the antennas on the aerodynamic performance of the Shell Eco-Marathon vehicle. Its aerodynamic performance is quantified in terms of the drag coefficient, velocity distribution and pressure distribution. The simulations were performed using ANSYS Fluent, utilising the $k-\varepsilon$ turbulence model to ensure a comprehensive coverage of flow behaviours across critical areas of the vehicle. The standard wall function approach was used to model potential turbulent flow around the vehicle body. Inflation layers were added to maintain a wall Y+ of around 30. Different element sizes were simulated and a mesh independence study was conducted. The setup that converged had a global element size of 0.02m, which produced an overall 23174519 number of elements, shown in Figure 39. The change in drag coefficient per element added was $-1.67503 \times 10^{-11}$, which satisfied the convergence criterion of $-1 \times 10^{-11}$.

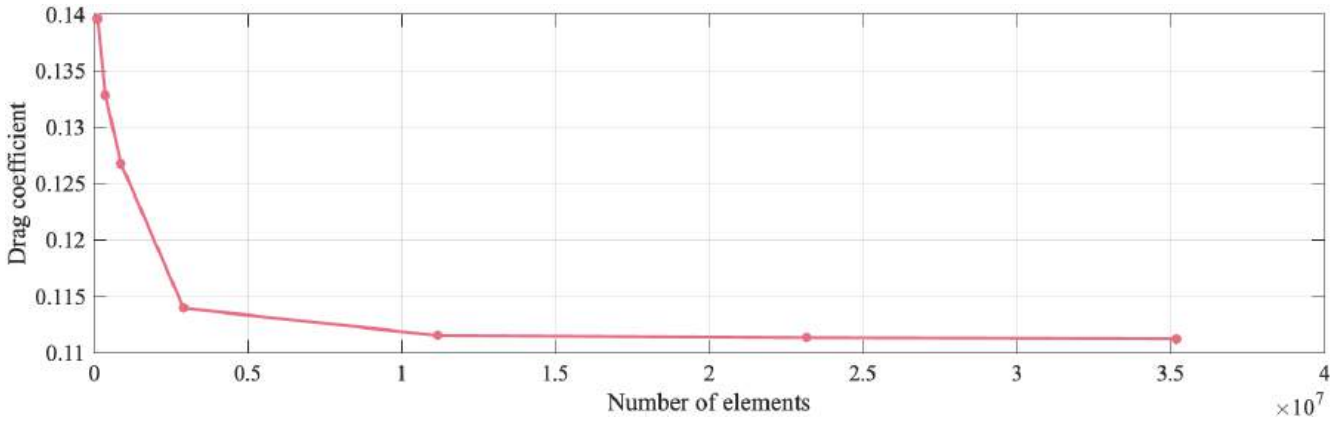


Figure 39: Mesh independence study.

### 5.1.1 Aerodynamic Drag

The drag coefficient $C_D$ is a dimensionless quantity that quantifies the drag or fluid resistance of an object in an environment such as air. It is given by the following equation:

$$C_D = \frac{2F_D}{A\rho_{\text{air}}v^2} \tag{1}$$

where $F_D$ is the drag force, $A$ is the reference area, $\rho_{\text{air}}$ is the density of air, $v$ is the velocity of the vehicle. $\rho_{\text{air}}$ is 1.225 kg/m$^3$ and $v$ is assumed to be the top speed of the vehicle, which is 11ms$^{-1}$.

The frontal area is used as the reference area $A$. The frontal area of the vehicle without the antennas, is 0.356 m$^2$. Whereas the frontal area of the vehicle with the antennas, as shown in Figure 40, is 0.3575 m$^2$.

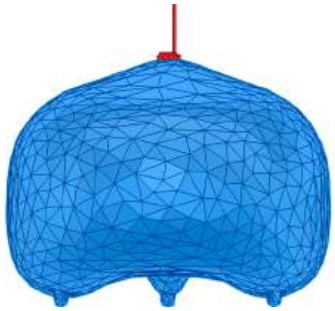

Figure 40: Reference area of the vehicle (blue) and antennas (red).

From the separate CFD simulations conducted with each CAD model, $F_D = 2.9373N$ for the vehicle without the antennas, and $F_D = 2.9525N$ with the antennas. The drag coefficient is found to be $C_D = 0.1113$ for the vehicle without an antenna and $C_D = 0.1141$ for the vehicle with the antenna. This shows that the antenna system causes a 2.5% increase in drag. The effect of this should be further evaluated with simulations along with real-world testing as there are exposed cables which are not modelled, this could potentially increase drag. These results were used for the computational model in MATLAB, covered in the data analysis Section 5.4.1.

### 5.1.2 Velocity field

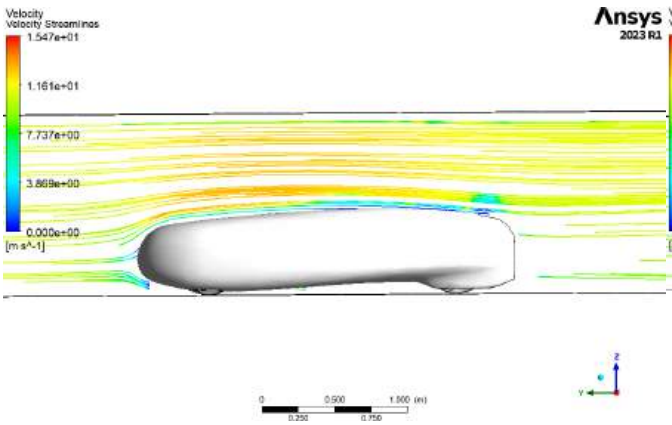


Figure 41: Velocity Distribution without Antennas.

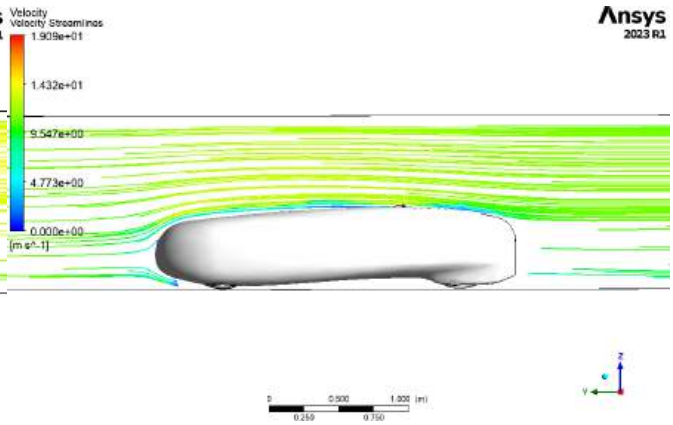


Figure 42: Velocity Distribution with Antennas.

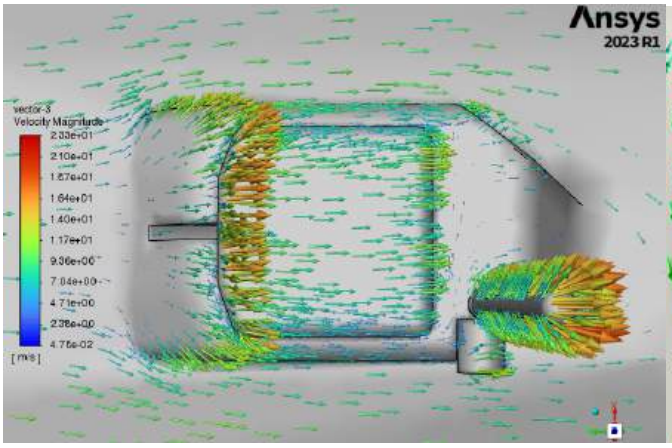


Figure 43: Top Surface of Antennas.

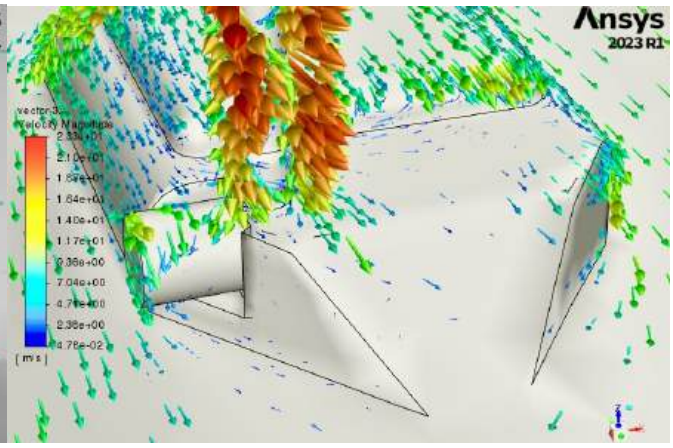


Figure 44: Rear of Antennas.

As seen in Figures 41 and 42, the velocity streamlines show a very similar distribution around the vehicle body despite having the antennas installed. The teardrop shape of the vehicle helps with flow attachment, as indicated smooth streamlines, parallel to the body contour. Furthermore, there is no turbulent flow at the wake region towards the rear of the vehicle. This demonstrates the successful aerodynamic design of the vehicle. There is a lack of a low-pressure area behind the vehicle which means that there is a minimal pressure difference between the front and the rear of the vehicle. This results in a reduction in the suction effect that pulls back on the vehicle which would otherwise increase drag. Figures 43 and 44 show that the majority of the air flows smoothly over the top surface of the antenna or around its sides. This is done with no disturbance to the flow field around the car, when compared to the original setup without the antenna. The GPS antenna, represented by the square-shaped block,

is short in vertical height, thereby minimally interrupting the airflow. In contrast, the radio antenna, characterised by its elongated rod-like structure, extends to a greater height. Nonetheless, its slender and cylindrical form allows air to flow past it without much velocity reduction. The side connection port of the radio antenna causes a slight flow disturbance, as evidenced by a localised reverse flow pattern. However, this is relatively minimal and vortexes do not form.

### 5.1.3 Pressure Field

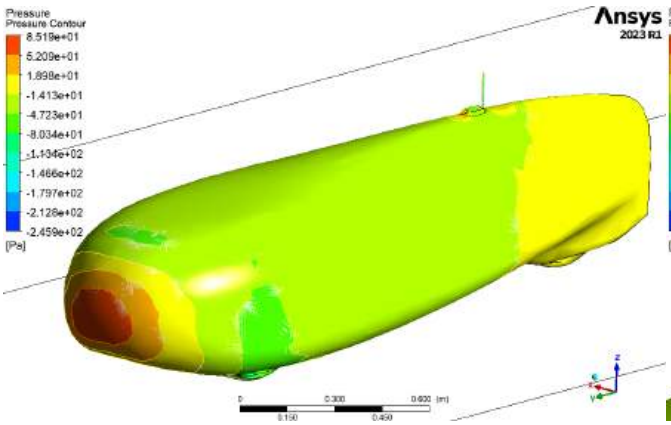


Figure 45: Pressure Distribution of Entire Vehicle.

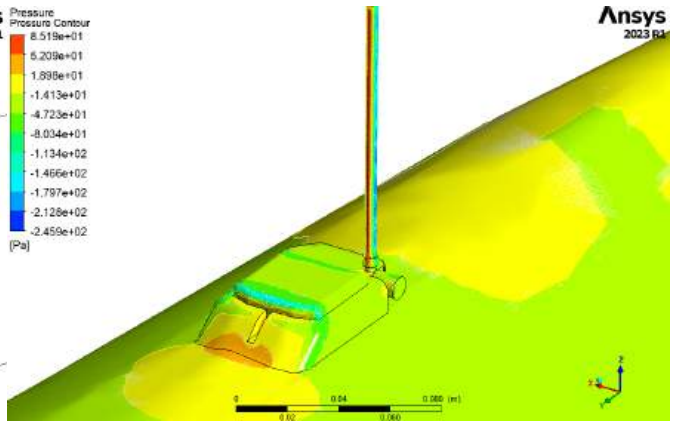


Figure 46: Pressure Distribution of Antennas.

It can be seen in Figures 45 and 46 that the vehicle experiences a maximum pressure of around 85Pa at regions facing perpendicular to the flow direction, which are situated at the front tip of the vehicle and the radio antenna. This is expected, as the direct impact from the airflow causes a stagnation point in the velocity field. At this point, the velocity of the airflow relative to the surface technically becomes zero. According to Bernoulli's principle, where the flow velocity is zero, the kinetic energy of the fluid particles is also zero. To conserve the total energy of the system, the pressure energy must increase. This conversion of kinetic energy into pressure energy at the stagnation point results in the highest static pressure, consequently causing the total pressure to increase at these regions, consequently resulting in an increase in drag force. The smooth shape of the vehicle significantly reduces high pressure regions. Similarly, the antenna system experiences very few high pressure regions, contributing to greater durability and longevity of the component as it is exposed to less stresses from the airflow. It also means that the antenna system will be able to take more accurate measurements. This is due to enhanced attachment stability, which reduces the risk of detachment or displacement from wind forces.

## 5.2 Testing

### 5.2.1 Radio Test

**Procedure:** Following the design of the radio, testing was done to identify the optimal setup of the radio parameters. The main parameters that were evaluated were the frequency used to send the radio message, the modulation type of the antenna, the data rate of sending, all as a function of distance between the two antennas. Three frequencies were tested, 433.05MHz, 433.95MHz, 434.79MHz. Three modulation types were used, FSK (Frequency Shift Keying), GFSK (Gaussian Frequency Shift Keying), and OOK (On OFF Keying). Three data rates were used, a low, medium, and a high one. For FSK and GFSK, these corresponded to 2, 57.6, and 250 Kbps. Whereas for OOK they were 2.4, 9.6, and 32 Kbps. Finally, the range started off at 50m and it was incremented until 500m. Setups were created by assigning a value for each of the previously listed four parameters. A test involves sending five batches of data, with each batch containing 100 messages of the maximum length of 58B. Following each test the following parameters were recorded for evaluation: the number of acknowledgements received from the receiver, the probability of a successful message transfer, the time taken to send the messages, the signal strength, and the average data rate.

Two separate tests were conducted. One with no height difference between the two antennas and another with a height difference of around 3m to simulate the actual race environment, the latter using a directional Yagi antenna.

This improved signal strength, hence increasing range. First, the in plane testing was performed to evaluate the system and narrow down the potential options, which were then further evaluated during the elevation test.

**Evaluation:** First, the three frequencies were tested at a distance of 50m. The antennas used were designed for 433.05MHz operation, hence the best results should be obtained using that frequency. Tests were done to verify this. The modulation type used was FSK with a data rate of 2Kbps. The main parameter that was considered when doing this test was the signal strength. As long as the message is received, a lower signal strength is desirable as it uses less energy to be transmitted. The test confirmed that 433.05MHz is the ideal selection for the system, and it will be used in all the following tests (Fig. 47).

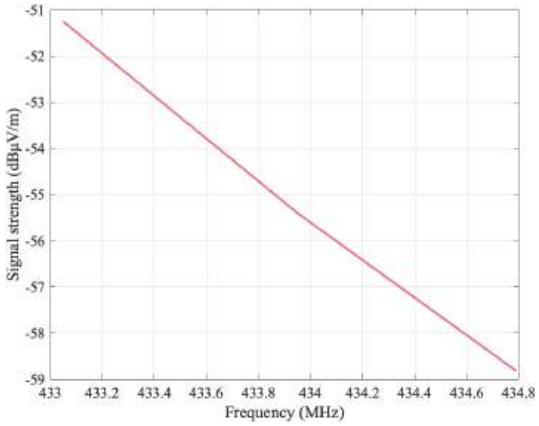


Figure 47: Signal strength as a function of frequency.

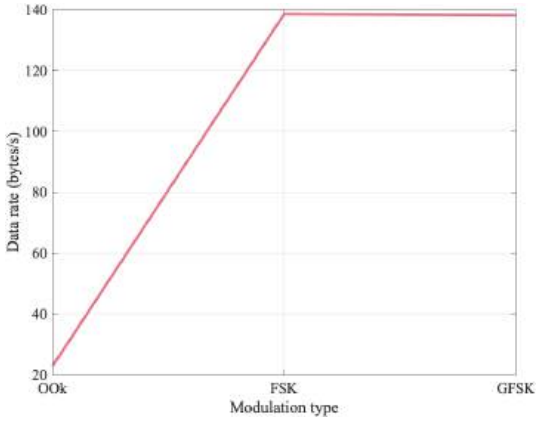


Figure 48: Data rates of various modulations.

Staying 50m apart, the three modulation options were tested, using their lowest data rate (Fig. 48). OOK displayed a considerably lower data rate along with having a low probability of a successful message transfer. After further investigation, it was decided not to continue testing OOK.

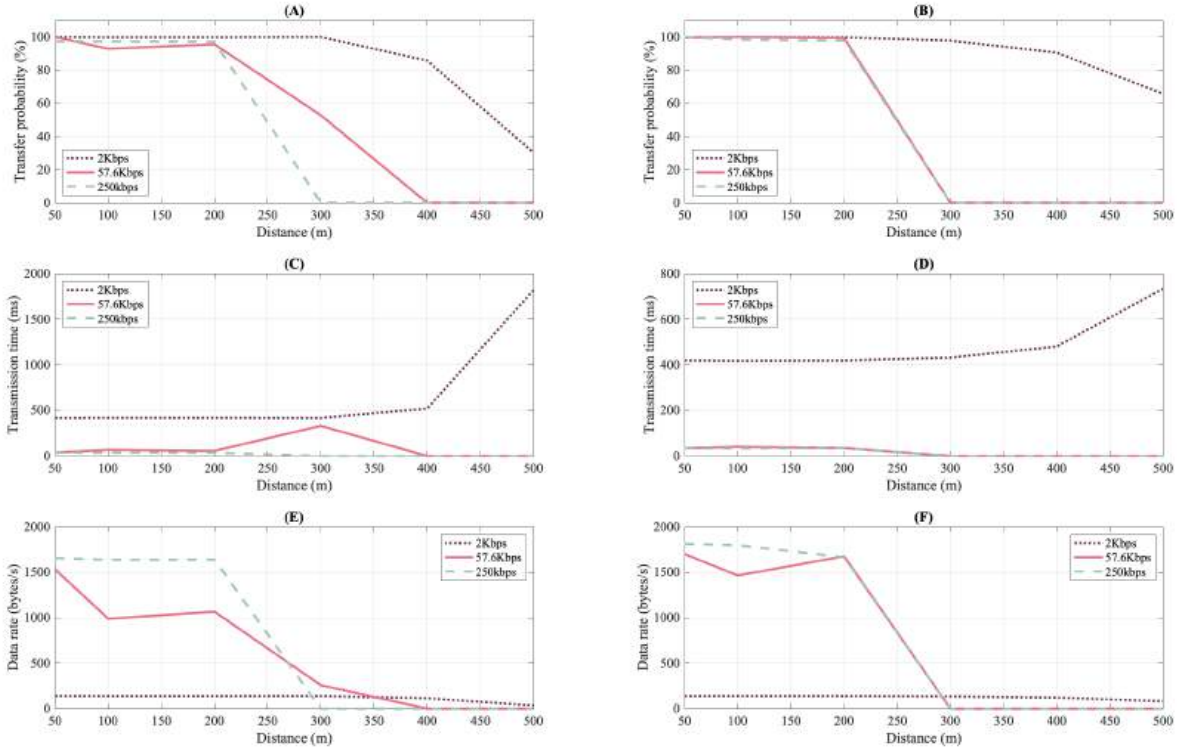


Figure 49: In plane test results with distance. (A) FSK message transmission probability, (B) GFSK message transmission probability, (C) FSK message transmission time, (D) GFSK message transmission time, (E) FSK average data rate, (F) GFSK average data rate.

The results in Figure 49 suggest that the lower the data rate, the higher the probability of successful message transmission over larger distances (plots (A) and (B)). However, this larger sending range comes with an increase in sending time (plots (C) and (D)). GFSK handles this increase much better compared to FSK. Higher data rates do not display this trend on the plots, because they exceeded the sending range from 200m onwards. Finally, higher data rates drop drastically at larger distances (plots (E) and (F)), this is once again due to their sending range being considerably lower compared to the 2Kbps data rate. The team would ideally use the highest possible data rate so that the message can be sent in the minimum amount of time. To further investigate whether using higher data rates is feasible, the team purchased a Yagi antenna. The test procedure was similar, however, there was an elevation difference to simulate the race conditions.

Using a Yagi antenna to receive the messages proved highly successful, as evidenced by Figure 50. Both the transmission probabilities (plots (A) and (B)) and the data rates (plots (C) and (D)) were adequately increased to cover more than the required 250m of range, which ensure that data does not stockpile during the race. However, the question still remained regarding which modulation to use FSK or GFSK. The key difference between FSK and GFSK is the transmission probability (Fig. 51). Due to the higher transmission probability, GFSK was selected.

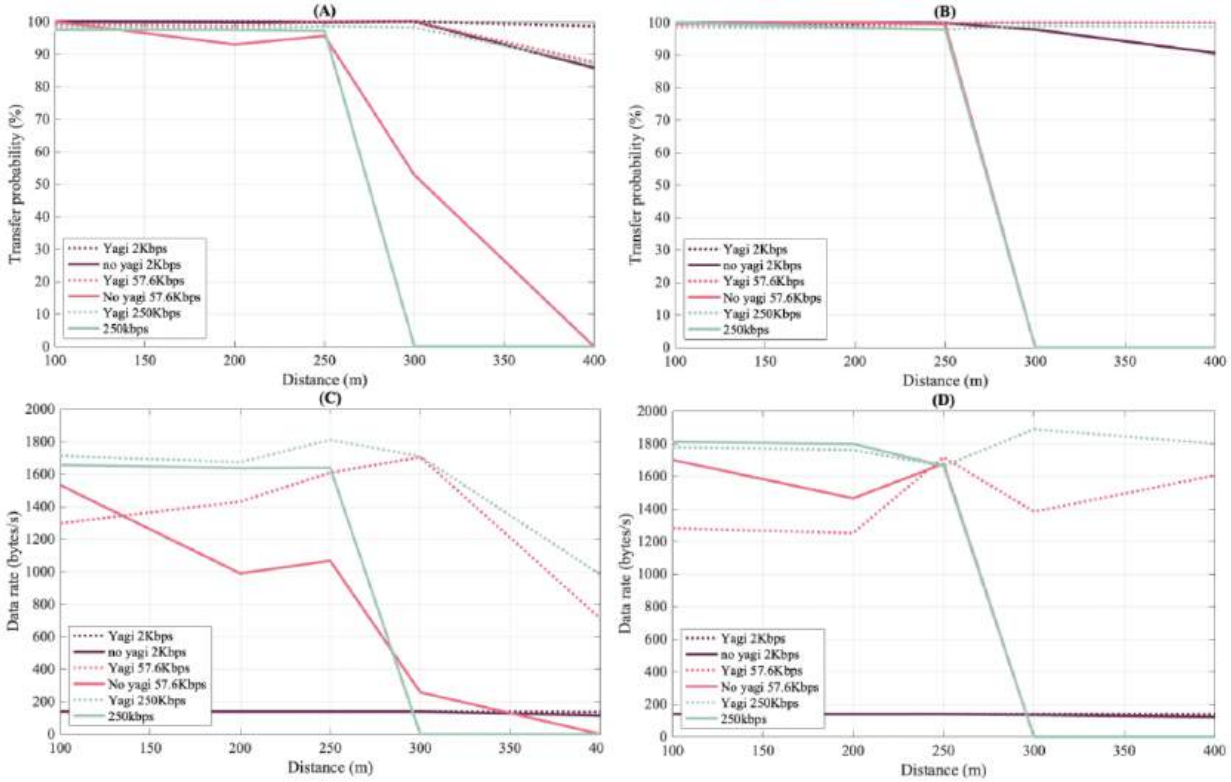


Figure 50: Comparison between Yagi and no Yagi test results. (A) FSK transmission probability, (B) GSK transmission probability, (C) FSK message data rate, (D) GFSK message data rate.

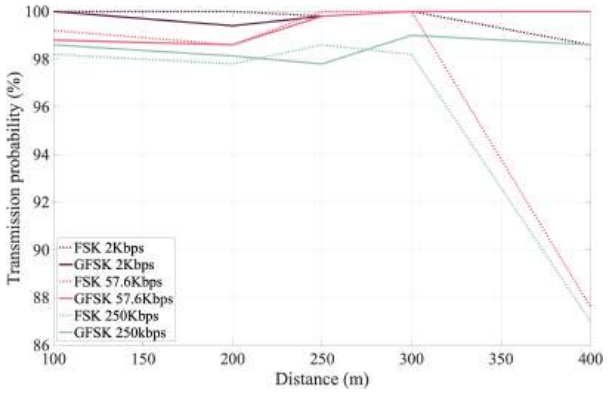


Figure 51: Comparison between FSK and GFSK.

**Conclusion:** The two antenna test that were conducted, reaffirmed the team about their design decision of going with RF communications to achieve wireless data transfer. From the first test, it became apparent that a Yagi antenna will be necessary to achieve a desirable range and data rate. A higher data rate is desired because it will mitigate risks related to aspects of the race that the team could not test for, such as the obstructions from the stands at the race, and the fact that the distance between the two antennas is constantly changing due to the vehicle going around the track. As a result, the team ended up selecting GFSK for the modulation type and 250Kbps for the data rate.

### 5.2.2 Bike Test

To deem the telemetry system ready for on-track testing, the GPS, IMU, Receiver Node and SD card reader were tested for reliability. These recorded the latitude, longitude, X Y Z axis accelerations and the timestamps. This was saved on the SD card to analyse the data. The system was mounted on a bike and tested in Regent's Park.

**Procedure:** Two different testing routes were proposed, a circular one to replicate the movement across a race-track, and a linear one to check for the GPS measurement's precision. For each route, three different attempts were conducted at different speeds. The first test was done at walking speed (1.5 m/s), the second at half the car's average speed (3.8 m/s) and the last attempt at the car's average competition speed (7 m/s). The two layouts are presented below in Figure 52 and Figure 53.

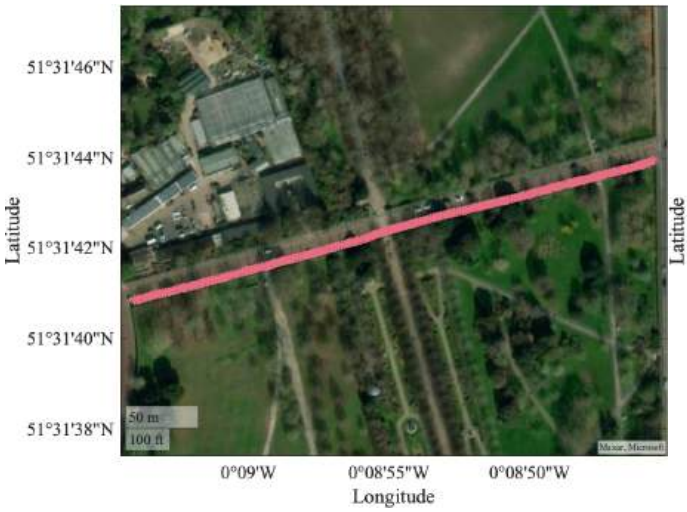


Figure 52: GPS Measurements for Straight at 1 m/s.

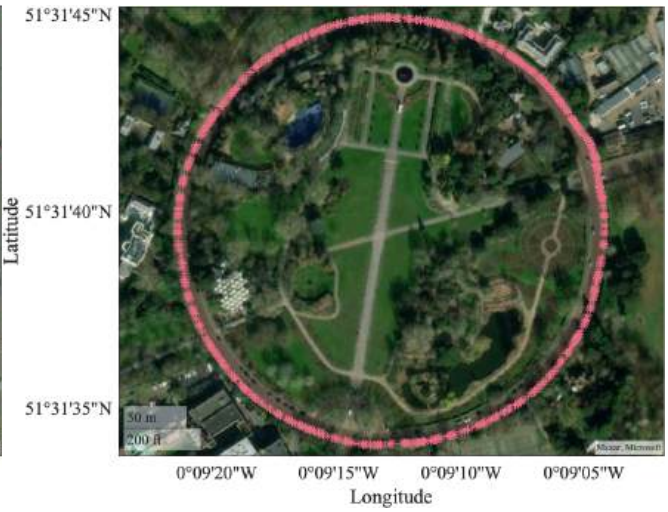


Figure 53: GPS Measurements for Circle at 7 m/s.

**Evaluation:** To analyse the raw data, a MATLAB script was written. The GPS measurements have shown great fidelity to the bike's moving pattern. No filtering was required for latitude and longitude. One important takeaway was the relationship between the bike's speed and the time between measurements. The resolution difference is visible between the two speeds. The number of measurements per lap is proportional to the speed. As a result, at 1.5 m/s, there were 31000 data entries on the SD card, compared to the 7500 data points for the lap matching the car's competition velocity. Therefore, the sensor writing frequency needs to be optimised to ensure that there are sufficient data points recorded to evaluate the car's performance, while minimising the data memory size.

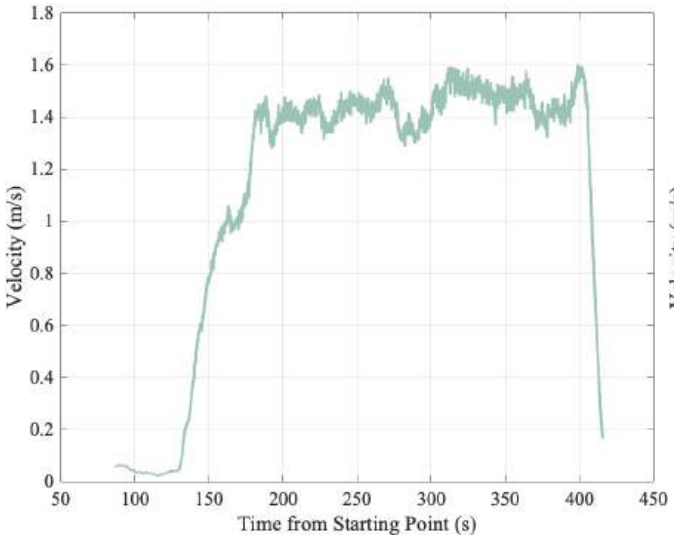


Figure 54: Velocity Data for Straight Path.

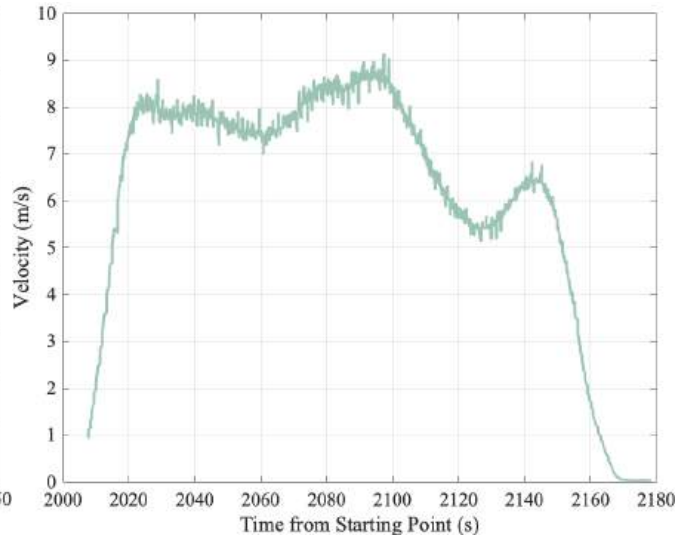


Figure 55: Velocity Data for Circle Path.

The MATLAB scripts were programmed to calculate the bike's velocity based on the GPS data and timestamps between measurements. The distance between two points can be obtained using the Haversine formula. Velocity is obtained from dividing the distance by the time taken to travel between the data points for each of the study cases:

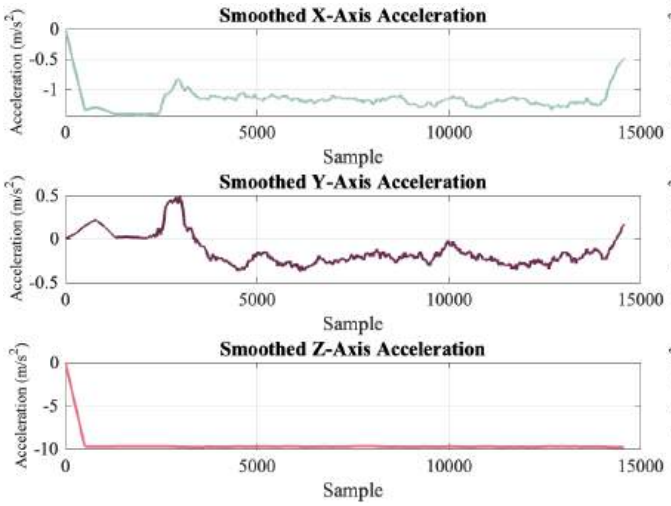


Figure 56: Acceleration Data for Straight Path.

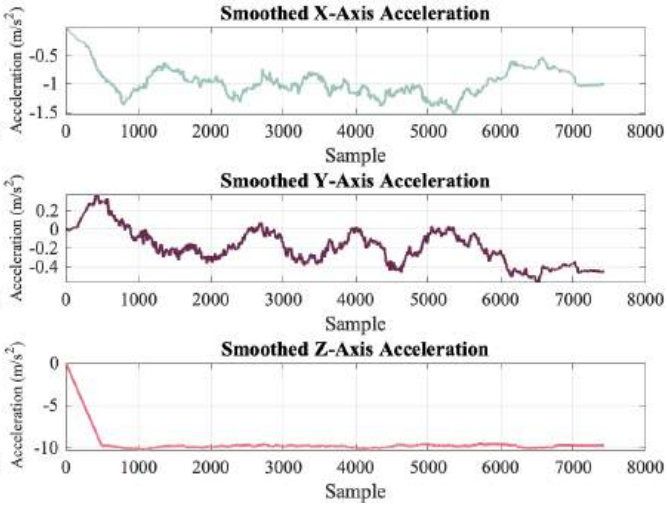


Figure 57: Acceleration Data for Circle Path.

The IMU data describes the car's acceleration across the X, Y, and Z-axes. The X axis is aligned perpendicularly to the car's movement. The Y axis is positioned along the bike's direction and the Z-axis is pointing vertically upwards. Unlike the GPS data, the acceleration requires a moving average filter to eliminate undesirable values. The measurements predict reliable output, confirmed by the constant Z axis readings at -9.81 m/s$^2$.

**Conclusions:** The data was compared and verified with available applications on smartphones. The telemetry system showed great fidelity to the phone measurements. In one instance, during the circle test at the car's competition speed, the phone GPS lagged, loosing an important number of data points. This marked a great success, as the telemetry system was developed to be more reliable than specialised phone applications.

### 5.2.3 On Track Testing

**Electric powertrain:** With all sensors having been tested before, the next chapter brought the telemetry system on-board with the car for several laps around CycloPark, a bike testing track outside London. The car was powered by electric batteries. The main goal of the test was to record data that would measure the car's energy consumption and identify driving patterns across the laps. The sensor measurements would be sent over wireless communication to the race engineer. The incoming live raw data was plotted to instruct the driver in real time on his performance.

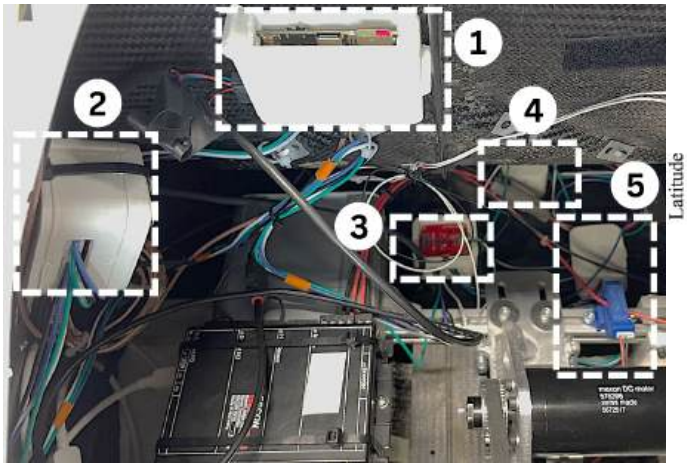


Figure 58: Sensor Placement during Electrical Test.


Figure 59: Measured Data Points around Cyclo Park.

The telemetry system sensors were placed as presented in Figure 58. It included the receiver (1), GPS (2), voltmeter (3), IMU (4) and the current meter (5). The SD card saved the car's latitude, longitude, velocity, X Y Z acceleration, voltage and current running through the battery and the pedal engagement. Figure 59 presents the total points registered for the testing sessions. Once again, the GPS measurements provided accurate readings of the car's position around the circuit.

**Procedure:** The test had the driver go anti-clockwise around the track for 15 laps. The car had to match the target lap time needed for the competition in Nogaro. Adjusting this for one lap's length around CycloPark, the driver had to complete one lap in less than one minute.

**Evaluation:** The overall raw testing data is depicted in Figure 60 and Figure 61. This is used to obtain an overview of the entire run. The Z-axis acceleration provides information about the track's elevation changes. A constant output shows there is little elevation change. The acceleration along the Y-axis measures the centrifugal force acting on the car while the X-axis shows the acceleration along the car's trajectory. The velocity graph depicts the driver's evolution throughout the testing session. Later laps denote an evolution of the driver's ability, higher speeds implying more confidence and better understanding of the manoeuvrability. The energy consumption evolution is overlayed. Higher speeds lead to a flattening trend in the car's power deployment.

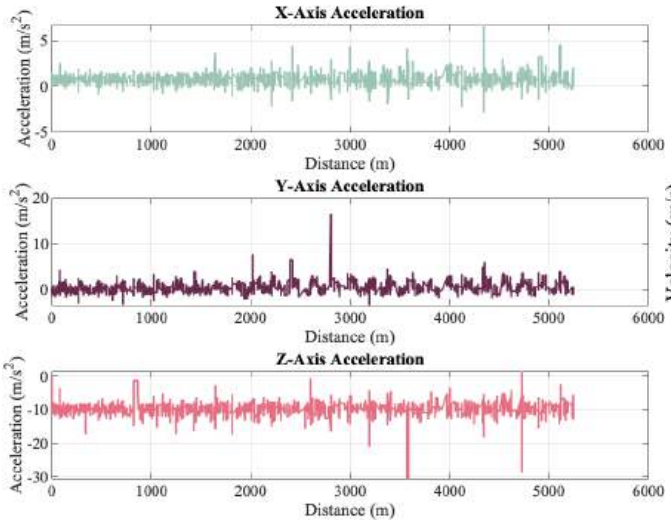


Figure 60: Testing IMU 3-axis Measurements.

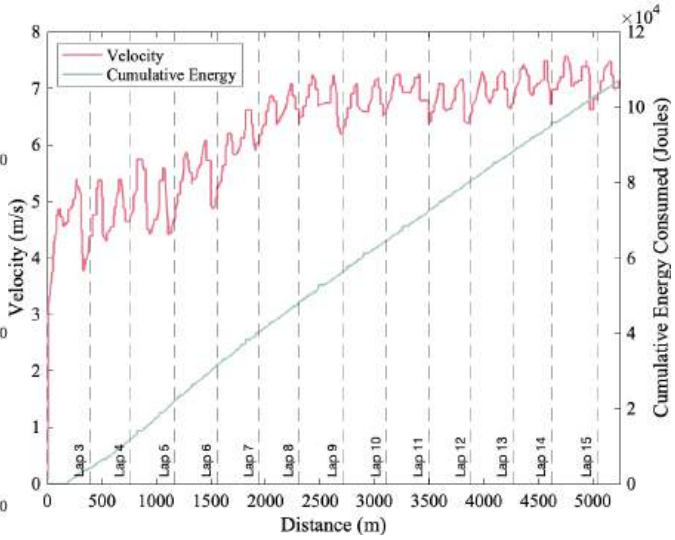


Figure 61: Testing Velocity and Energy vs Distance.

Processing is required to transform raw data into meaningful information. The first task of the MATLAB program is to obtain an overview of each of the measured laps. A geo-fence is set for the start/finish line to separate the runs. Then, the mentioned sensor data is processed to obtain key performance indicators: the measured distance within a lap, the car's energy consumption, competition rating in terms of km/kWh, lap time and average speed. A table is then generated automatically that sorts the laps in terms of competition rating. This output is depicted in Table 14. This is then used to assess which laps can be further analysed to identify driving patterns that optimise the racing strategy. Laps 1, 2 and 3 have corrupted data. The GPS, Voltmeter and Current meter took longer to configure and save data reliably. As a result, their energy consumption and position tracking are missing. This was spotted looking at the energy trend, which only started recording half-way through the third lap. To be within the competition target lap time, a lap around CycloPark needs to be completed within a minute. Therefore, laps 14 and 15 represent the best performance of the driver. The MATLAB program also lists an overview of the entire session. The total distance covered was 5243.44 meters, the average velocity was 5.67 m/s, the total energy consumed was 0.03 kWh and the overall efficiency rating was 175.60 km/ kWh.

Table 14: Testing Data Measured at CycloPark, UK.

| Lap | Distance (m) | Energy (J) | Rating (km/kWh) | Time (s) | Average Speed (m/s) |
|---|---|---|---|---|---|
| 3 | 408.82 | 4283.3 | 343.61 | 94.246 | 4.3378 |
| 15 | 370.45 | 7161.6 | 186.22 | 52.603 | 7.0423 |
| 14 | 400.97 | 7821.9 | 184.55 | 57.214 | 7.0083 |
| 4 | 374.44 | 7499.6 | 179.74 | 73.3 | 5.1083 |
| 11 | 390.1 | 7912.3 | 177.49 | 57.429 | 6.7928 |
| 13 | 379.68 | 7769.2 | 175.93 | 55.595 | 6.8295 |
| 12 | 385.13 | 7881.5 | 175.92 | 57.233 | 6.7292 |
| 10 | 386.68 | 7989.5 | 174.23 | 57.803 | 6.6896 |
| 8 | 378.51 | 7854.2 | 173.49 | 56.759 | 6.6687 |
| 9 | 388.03 | 8207.6 | 170.2 | 58.227 | 6.664 |
| 7 | 387.57 | 8869.1 | 157.32 | 65.532 | 5.9142 |
| 6 | 396.19 | 9582.6 | 148.84 | 73.698 | 5.3759 |
| 5 | 392.62 | 10427 | 135.55 | 80.535 | 4.8751 |
| 1 | 0.94764 | 0 | -Inf | 1.129 | 0.83936 |
| 2 | 4.7923 | 0 | -Inf | 66.707 | 0.071842 |

**Conclusion:** The test was successful as the car was transmitting and storing sensor data, confirming the project's proof of concept. The telemetry system recorded a wide range of information that described the car's movement on track and energy deployment across it. The recorded information was further analysed to aid driver improvement and chassis optimisation. However, it also highlighted further areas of improvement for the upcoming testing sessions. The GPS and throttle potentiometer had system integration issues. The GPS recordings were only registered past the 3rd lap, while the throttle was not functioning for the entirety of the test. This was due to an electrical issue that interfered with the car's motor engagement. Further in-house testing was conducted with the car being run on roller's to accommodate these issues. The GPS code was debugged, while the throttle was redesigned. The throttle measurements provide information in regard to where the car is accelerating and not. As this was not available from this test, the data analysis algorithm was adjusted to determine these regions based on velocity gradient.

**Hydrogen powertrain:** The last test before the competition in France had the car run on hydrogen around CycloPark. The goal was to monitor the hydrogen powertrain and configure the motor controller to ensure a good balance between energy usage and on-track speed. The data analysis followed the same methodology as the battery electric test, including tables summarising the car's lap-by-lap performance and comparison between laps. The following section will detail the additional analysis required for a hydrogen power train.

**Procedure:** Aided by the LCD interface displaying the supercapacitor SOC, the driver drove around track anti-clockwise for 7 laps to match a time of 1 minute per lap. Wireless data from the car was transmitted and displayed to the race engineer to monitor the status of the fuel cell and guide the driver's performance on track. Table 15 highlights the output of the MATLAB program that sorts the attempts in order of energy efficiency. As opposed to the electrical test, the hydrogen powertrain exhibits large variations in lap energy consumption.

Table 15: Testing Data Measured at CycloPark, UK.

| Lap | Distance (m) | Energy (J) | Rating (km/kWh) | Time (s) | Average Speed (m/s) |
|---|---|---|---|---|---|
| 5 | 392.34 | 4283.2 | 329.93 | 58.559 | 6.6999 |
| 6 | 395.2 | 5146.92 | 276.62 | 138.81 | 2.8471 |
| 1 | 387.89 | 6433.52 | 216.92 | 65.065 | 5.9616 |
| 4 | 390.59 | 8572.68 | 164.03 | 57.475 | 6.796 |
| 7 | 202.86 | 4520.16 | 161.57 | 143.14 | 1.4172 |
| 3 | 395.98 | 10353.6 | 137.69 | 58.559 | 6.7621 |
| 2 | 383.91 | 12611.16 | 109.59 | 58.559 | 6.5559 |
| 0 | 201.64 | 18550.52 | 39.217 | 559.56 | 0.36036 |

**Evaluation:** The telemetry system was improved to mitigate the issues highlighted in the previous sessions. The throttle voltmeter was recalibrated and the data was stored successfully to monitor the pulse and costing distances across the lap. The spikes in voltage present in Figure 62 indicates when the car was accelerating. From this, the total energy and motor engagement can be estimated. Matching it with the GPS location, the pulsing and coasting regions can be found. The hydrogen powertrain requires a strategic deployment of the supercapacitor's energy. Hence, careful monitoring is required so that they do not run out of energy faster than they can recharge. For the test, the supercapacitor SOC dependency over time has been depicted in Figure 63.

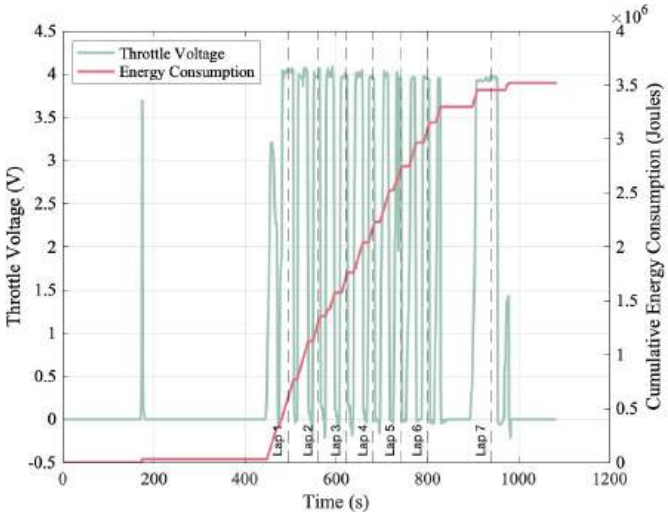


Figure 62: Throttle and Energy Dependency over Time.

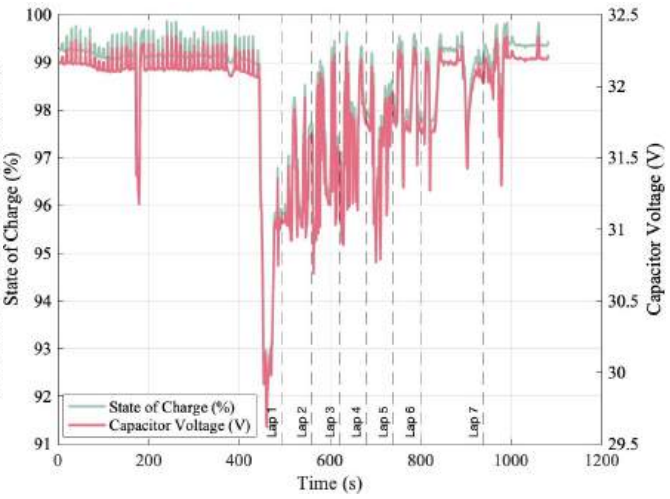


Figure 63: Pulsing and Coasting Regions.

**Conclusion:** This test confirmed that the system is compatible with both the electric and hydrogen powertrain. This setup was used in the Shell Eco-marathon competition in the 2024 season. Furthermore, the improvements in measurement reliability and visualisation methods were confirmed.

## 5.3 System Setup and Evaluation

### 5.3.1 System Weight

From several design iterations of the PCBs and casings, the total weight of the system inside the vehicle was minimised to 999g. It can be seen from Table 16 that the majority of the weight consists of the display.

Table 16: Weight of the system inside the vehicle (internal) and outside the vehicle (external). (nc = node computer)

| **Component - Inside the vehicle** | **Case Weight (g)** | **Electrical Weight (g)** | **Total Weight (g)** | **Amount** | **Overall Weight (g)** |
|---|---|---|---|---|---|
| GPS (nc) | 26 | 16 | 42 | 1 | 42 |
| External antennas | 22 | 140 | 162 | 1 | 162 |
| Screen (nc) | 24 | 14 | 38 | 1 | 38 |
| Display | 106 | 178 | 284 | 1 | 284 |
| IMU (nc) | 25 | 16 | 41 | 1 | 41 |
| Power meter (nc) | 24 | 15 | 39 | 5 | 195 |
| Receiver | 19 | 26 | 45 | 1 | 45 |
| Wires | - | - | 24 | 8 | 192 |
| **Component - Outside the vehicle** | | | | | |
| Ground station | 8 | 16 | 24 | 1 | 24 |
| | | | **System Total Weight - Inside the vehicle:** | | 999 |

### 5.3.2 System Energy Consumption

The telemetry system inside the vehicle is powered by 5V and the numerous sensors draw different levels of current, which are summarised in Table 17. The total current drawn by the system is 1030mA, which gives a total power draw of 5.65W. The competition strategy target time for the race is 36 minutes and 33 seconds. Therefore, it is determined that the total energy required to run the telemetry system is 12390J. Analysing for the performance exhibited on lap 14 during the testing session, the telemetry system amounted for 3.73% of the total energy consumption. Without it, the car would have scored an efficiency rating of 191.42 km/kWh instead of 184.54 km/kWh.

To mitigate the problem of high power consumption, different system configurations can be used by removing certain components, owing to the modular design. The practice sessions require the entire telemetry system to maximise driver preparation. During initial official attempts, the telemetry system would be simplified by removing the screen, as it amounts to 71% of its energy consumption. This will reduce its energy expenditure down to 3618J for the entire race, amounting to 1.09% of the total energy consumption of the vehicle, increasing the vehicle's efficiency rating to 186.57 km/kWh. Later runs would only use the data storage and gathering system. At this point, the driver should be familiar with the track. The race engineer will keep track of lap times using a stopwatch to instruct the driver on the remaining lap time. This new system without the screen and wireless communication will only take up 2521.86J for the entire race, consuming 0.76% of the total vehicle energy usage. This cost is worth the benefits of analysing the lap data. The efficiency rating will increase to 189.97 km/kWh.

It is important to note that since the ground station is connected to the race engineer's laptop, it does not draw energy from the vehicle. Its weight and power requirement is summarised in Table 16 and Table 17. In addition, removing the components would cause a reduction in system weight, further enhancing the energy rating of the vehicle. Moreover, considering the system without the display FOCs 6.5.0 and 6.6.0 are met. Compared to commercially available options, this system is 95.5% lighter, and consumes 90% less energy [22–24]. The receiver weighs 45g and requires 0.5W of power. However, with the display installed, the system uses 5.65W of power, which does not satisfy FOC 6.6.0.

Table 17: Power of the system inside the vehicle (internal) and outside the vehicle (external). (nc = node computer)

| **Component - Internal** | **Current (mA)** | **Voltage (V)** | **Power (W)** | **Amount** | **Total Power (W)** |
|---|---|---|---|---|---|
| GPS (nc) | 30 | 5 | 0.15 | 1 | 0.15 |
| Screen (nc) | 20 | 5 | 0.1 | 1 | 0.1 |
| Display | 800 | 5 | 4 | 1 | 4 |
| IMU (nc) | 30 | 5 | 0.15 | 1 | 0.15 |
| Power meter (nc) | 30 | 5 | 0.15 | 5 | 0.75 |
| Receiver | 100 | 5 | 0.5 | 1 | 0.5 |
| **Component - External** | | | | | |
| Ground station | 40 | 5 | 0.2 | 1 | 0.2 |
| | | | **Total Power - Internal:** | | 5.65 |

## 5.4 Race Strategy through Data Analysis

### 5.4.1 Post-Practice Analysis

The recorded sensor data on the SD card is analysed post-race to prepare the driver for upcoming competition runs. The following methodology can be used at Nogaro to highlight efficient driving patterns. The MATLAB program was used to compare better and worse attempts around CycloPark for the electric and hydrogen powertrains.

**Hydrogen powertrain velocity and energy trends:** An important observation can be made regarding the role of the discharging and charging behavior of the supercapacitors in optimising the fuel efficiency. Figure 65 presents the velocity profile of the car on two different laps of a 7-lap test run. Although the speed trends correlate well, the energy consumption between the two laps varies drastically, lap 3 having consumed two times more energy.

This variation can be observed in Figure 64. Compared to lap 5, lap 3 has numerous spikes in energy deployment, with the supercapacitors charging and discharging rapidly across the lap. To mitigate this issue, the driver will be instructed to accelerate gradually, to ensure a smooth transition between the operational periods.

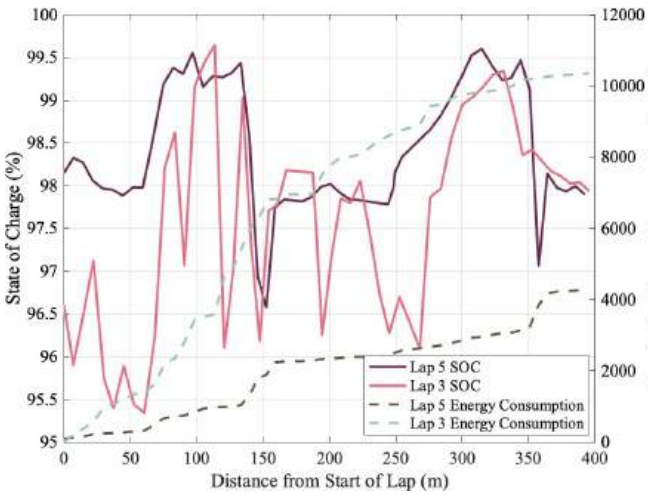


Figure 64: SOC and Energy Consumption over Time.

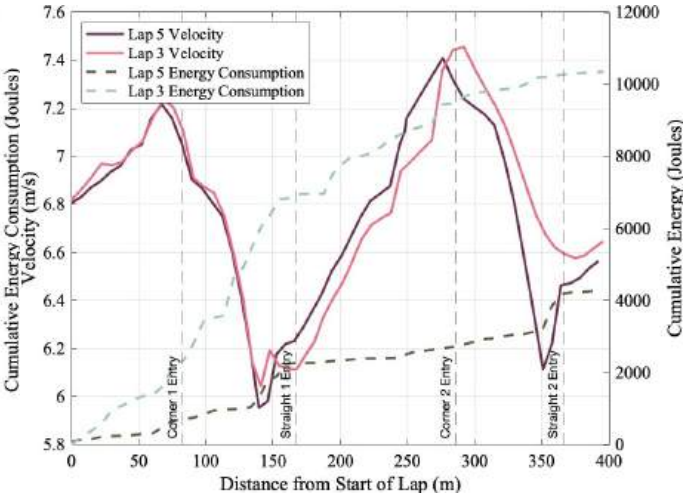


Figure 65: Velocity and Energy Consumption over Time.

**Electric powertrain velocity and energy trends:** The MATLAB program first plots the two laps' race line around the track from the saved geographical data. This is depicted in Figure 66. Lap 6 follows a wider corner line, while lap 14 goes closer to the apex. The velocity and energy trend of these laps are plotted in Figure 67. As shown in Table 14, lap 14 is the more efficient one. Higher speeds were achieved in this lap as well. Figure 67 shows a more interesting trend in energy consumption. One important take-away is in the car's energy expenditure during pulsing and coasting periods. There is little drop in power usage across the two stages, the car using a considerable amount of energy even while coasting. As a result, lap 14 is more efficient.


Figure 66: Lap 14 and 6 Race Line Comparison.

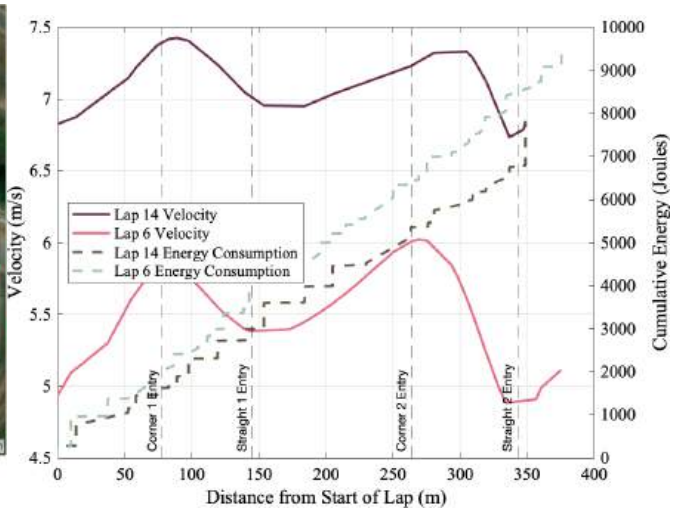


Figure 67: Lap 14 and 6 Speed and Energy Trends.

Comparing the two velocity trends, it can be noted that the driver was pulsing up until the apex of the second corner, whereas in lap 6, this stopped at the entry. This insight allows the driver to build up their confidence around the track, identifying how far into the corner they were able to accelerate and how much speed is possible to carry. The pulsing and coasting deployment are monitored using the throttle sensor data, plotted in Figures 68 and 69.


Figure 68: Lap 14 Pulsing and Coasting Strategy.


Figure 69: Lap 6 Pulsing and Coasting Strategy.

**Energy losses:** More data and race strategy insights can be extracted from the accelerometer mounted in the car. Figures 70, 71 depict the comparison of acceleration along the X-axis and Y-axis through the two laps. The X-axis acceleration is oriented along the car's forward movement. This can be used at Nogaro to determine the overall acceleration across the different velocity ranges and slopes to optimise the team's computational models. The Y-axis acceleration is of particular interest as it relates to the car's stability around a corner and the driver's handling of the prototype. Spikes in Figure 71 allow for the localisation of corners on the track. The Y-axis acceleration measures the centrifugal force acting on the car. This is used to calculate the slip angle while turning.

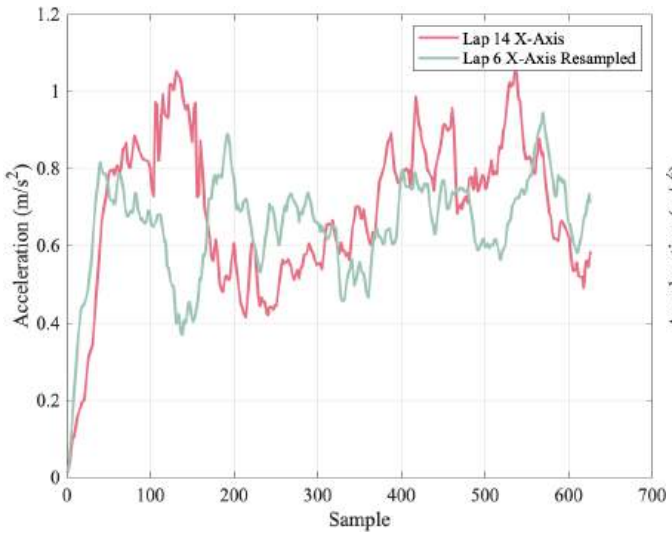


Figure 70: X-axis Acceleration Comparison.

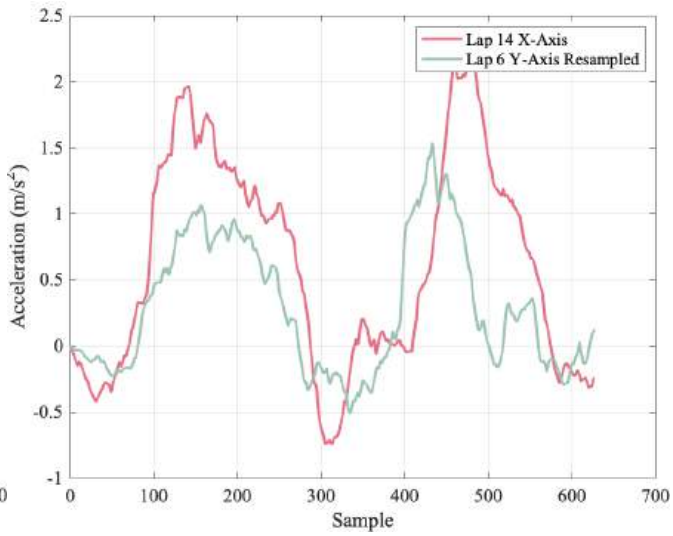


Figure 71: Y-axis Acceleration Comparison.

As the car turns into a corner, the centrifugal force is pulling the car away from its wheel's trajectory. This results in a mismatch between the tyre's orientation and the car's movement. The difference in angle between the two is called the slip angle. The rolling resistance and cornering stiffness counter the action of the centrifugal force. These result in energy losses as they act as a resistive force. Further energy is lost due to aerodynamic drag, electrical and mechanical losses within the car's powertrain. To evaluate these losses, the car is studied after the uni-cycle model. The Free-Body Diagram is shown in Figure 72.

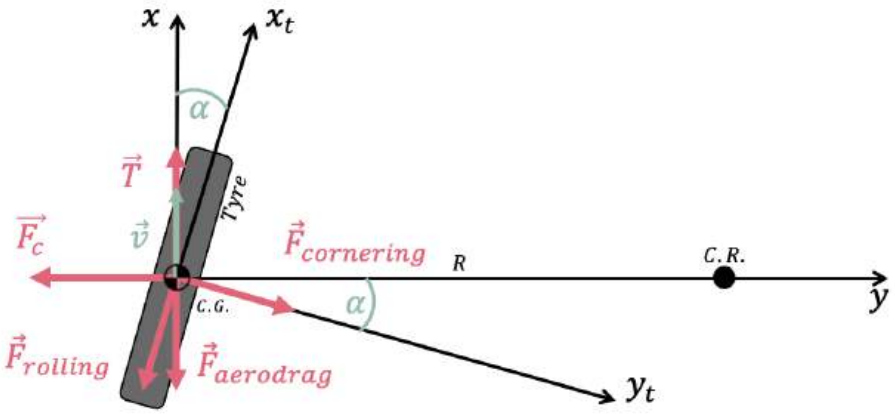


Figure 72: Free Body Diagram of the Car Modelled as a One Tyre System.

The slip angle ($\alpha$) is related to the tyre drag, the wheel exhibiting rolling resistance and cornering stiffness while turning. The rolling resistance ($F_{\text{rolling}}$) is the longitudinal frictional force acting at the contact surface between the tyre and road. The cornering stiffness ($F_{\text{cornering}}$) is the perpendicular resistive force at the contact surface between the tyre and the road. Due to the small velocity and wide turning arc in a corner, the slip angle is unlikely to reach over 5°. The two drag forces can be calculated as follows using the small angle approximation:

$$F_{\text{rolling}} = f_R M g \tag{2}$$

$$F_{\text{cornering}} = C_\alpha \alpha \tag{3}$$

where $f_R$ is the tyre's friction coefficient, $M$ is the total mass of the system taking into account the driver's mass ($m_{\text{driver}}$) and the car's mass ($m_{\text{car}}$), $g$ is the gravitational acceleration and $C_\alpha$ is the tyre cornering stiffness coefficient. The remaining forces are the tractive force ($T$), the centrifugal force ($F_c$) and the aerodynamic drag ($F_{\text{aerodrag}}$). These can be expressed as follows:

$$T = \frac{P}{v} \tag{4}$$

$$F_{\text{aerodrag}} = \frac{1}{2} C_D \rho A v^2 \tag{5}$$

$$F_{\text{c}} = M a_y \tag{6}$$

where $P$ is the motor power, $v$ is the car's velocity, $C_D$ is the car's drag coefficient in air, $\rho$ is the density of air, $A$ is the frontal area and $a_y$ is the centripetal acceleration. As mentioned before, the IMU Y-axis reading is the centripetal acceleration. All other coefficients have been determined experimentally by the UCL Shell Eco-marathon team [4][29]. The values for $C_\alpha$ and $f_R$ depend on the tyre's pressure. It has been found that the optimal performance is achieved at 80 bar, as the cornering stiffness coefficient is minimum. All model parameters are listed in Table 18:

Table 18: Model Parameters.

| **Parameter** | $m_{car}$ (kg) | $m_{driver}$ (kg) | $P_{motor}$ (W) | $A_{car}$ ($m^2$) | $C_D$ | $f_R$ | $C_\alpha$ |
|---|---|---|---|---|---|---|---|
| **Value** | 45 | 55 | 350 | 0.39 | 0.1323 | 0.0027 | 0.221 |

The total energy consumption during the lap was determined from the voltmeter and current meter. Rolling resistance, cornering stiffness and aerodynamic drag are determined by taking into account the car and wheel properties, as well as the recorded sensor data relating to its movement around the lap. The slip angle can be found from the force equilibrium along the Y-axis present in Figure 72:

$$F_c + F_{rolling} sin(\alpha) - F_{cornering} cos(\alpha) = 0; \tag{7}$$

The small angle approximation gives:

$$sin(\alpha) = \alpha \tag{8}$$

$$cos(\alpha) = 1 \tag{9}$$

Introducing (8) and (9) into (7) and then rearranging for the slip angle gives:

$$\alpha = \frac{Ma_Y}{C_\alpha - f_R Mg} \tag{10}$$

The energy losses between two data points can be calculated by multiplying the resistive forces acting along the car's trajectory by the distance in between two data points. To calculate the energy losses due to rolling resistance (11), cornering stiffness (12) and aerodynamic drag (13), the following formulas are implemented in MATLAB:

$$E_{\text{rolling}} = \sum_{i=2}^{i=n} F_{rolling} cos(\alpha) d(i, i-1). \tag{11}$$

$$E_{\text{cornerning}} = \sum_{i=2}^{i=n} F_{cornering} sin(\alpha) d(i, i-1). \tag{12}$$

$$E_{\text{aerodrag}} = \sum_{i=2}^{i=n} F_{aerodrag} d(i, i-1). \tag{13}$$

where d(i,i-1) is the Haversine formula to calculate the distance between two consecutive points $i$ and $i-1$ based on their latitude and longitude measurements. Once determined, the electrical and mechanical losses are calculated by subtracting all drags from the total measured energy consumption. Figures 73 and 74 detail the energy losses of both attempts as follows:

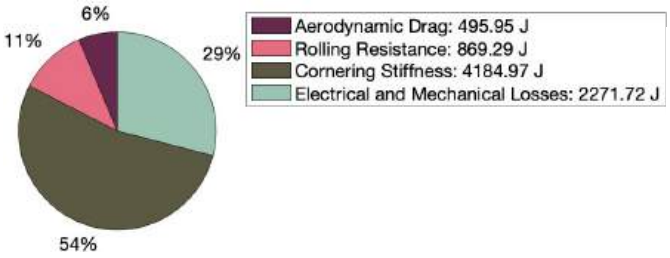


Figure 73: Lap 14 Energy Losses.

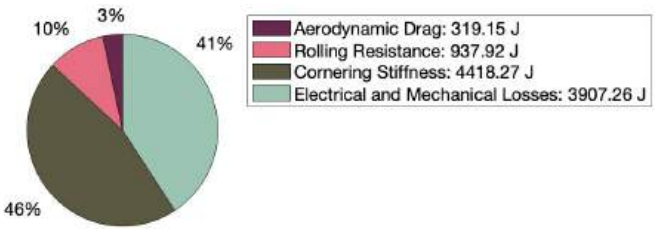


Figure 74: Lap 6 Energy Losses.

The tyre losses are positively correlated with the slip angle. These can be minimised by instructing the driver to gradually turn in a corner to avoid rapid increases in centrifugal forces and tyre drag. As a result, the Y-axis acceleration allows the driver to identify lap patterns with improved cornering strategy that minimise the rolling resistance and cornering stiffness. Sudden spikes denote rapid manoeuvres and changes in direction that increase the energy losses.

The most significant energy loss comes from cornering resistance. The second-highest loss is noticed in electrical and mechanical losses across the two laps. However, in lap 14, electrical losses are 42% lower than the ones in lap 6. This points back to the noticed pattern in the laps' energy consumption and losses during coasting. This can be an area to investigate in Nogaro. The driver will be instructed to increase the speed as much as possible without needing braking. Consequently, the lap times will decrease. Their energy consumption will be monitored to identify whether shorter lap times lead to better results, as the coasting period does not reduce significantly the energy consumption. This also highlights the need to emphasise on powertrain development and programming of the motor controller to optimise the power output.

### 5.4.2 Competition Preparation

The optimisation process is iterative. To extract the car's best performance, more testing data was analysed in the team's preparation for the competition. The insight into the power consumption during pulsing and coasting periods from the previous analysis encouraged the team to improve the design of the powertrain. This led to the acquisition of a new Maxon motor which is 95% efficient. The previous motor was only 78% efficient. Therefore, the team is estimating that the new powertrain electrical losses will decrease by at least 21%. Introducing this to the energy loss algorithm, the efficiency is expected to increase by 10%.

The current target lap time at Nogaro identified a conservative completion time per lap of 218.37 seconds. This left an error margin of 1 minute and 37 seconds that should accommodate for the presence of other cars on the track. However, the present testing dataset highlights the need for further optimisation of the target lap time due to the high energy cost of coasting periods. Upcoming tests will investigate this issue and a new target lap time will be determined. To ensure that the driver adheres to the strategy, a lap timer is displayed continuously on the screen. The driver interface is designed to observe the accumulation of time losses to obtain a delta comparing current performance to the target lap time. The most time is lost on the starting lap, as the car needs to build up the pace from a standstill. The hydrogen powertrain is monitored through the supercapacitor SOC which informs the driver of the available energy. This is needed by the driver to determine whether overtaking is safe improving the driver's safety (FOC 5.2.2).

### 5.4.3 Race Strategy Development

UCL's Shell Eco-marathon car will be running on hydrogen at the competition in France. The chosen driving strategy is pulsing and coasting. No braking is to be used during the race within safe driving conditions as this results in a loss of useful energy. The proposed data analysis methodology was used in a collaboration with the team to determine the race strategy at the competition. This has been adapted to the requirements of a hydrogen powertrain, and simulation analysis was done to correspond with the analysis undergone for the hydrogen configuration.

The only available data from the previous competition was a live recording of the driver's most successful attempt. Upon further investigation, the motor engagement was audible, allowing for the prediction of pulsing and coasting regions and timings along the track. In the coming season, this will be done automatically by the data analysis system prepared by the team. This insight was used by the UCL team to develop a simulation of the hydrogen powertrain and its power deployment around the track given the proposed strategy. The results give the current and voltage trend across the track. Our analysis provided insights into the expected energy consumption and lap-by-lap behaviour of the simulated car.

Firstly, the energy consumption is estimated for the entire race, shown in Figure 75. The estimated energy at the end of the race is 258842 Joules, leading to an energy rating of 218.357 km/kWh. The team's simulations provide estimations of the current running into the motor for one lap. This is depicted in Figure 76.

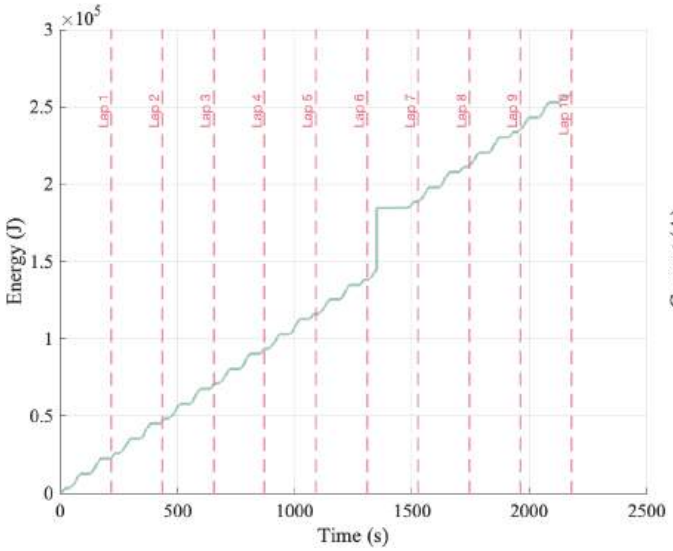


Figure 75: Nogaro Energy Consumption Simulation.

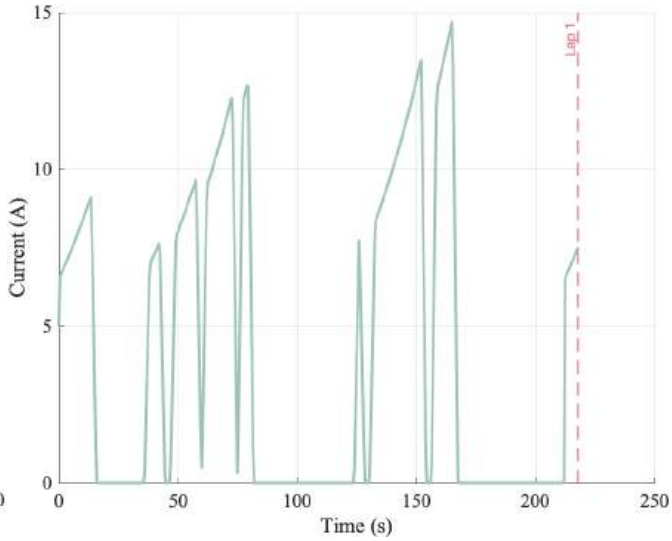


Figure 76: Nogaro One Lap Current Deployment.

Spikes in current represent throttle engagement and acceleration, while no current represents coasting. This driving behaviour is strongly linked with the configuration of the powertrain. The simulation done by the UCL team also provided calculations for the supercapacitor SOC and the State of Energy (SOE), which otherwise would be measured by the telemetry system. The supercapacitor's state of charge is influenced by the car's acceleration. These need to be monitored to ensure safe operation during the competition. The data analysis provided a platform to monitor the simulation results. This has been depicted in Figures 77 and 78.

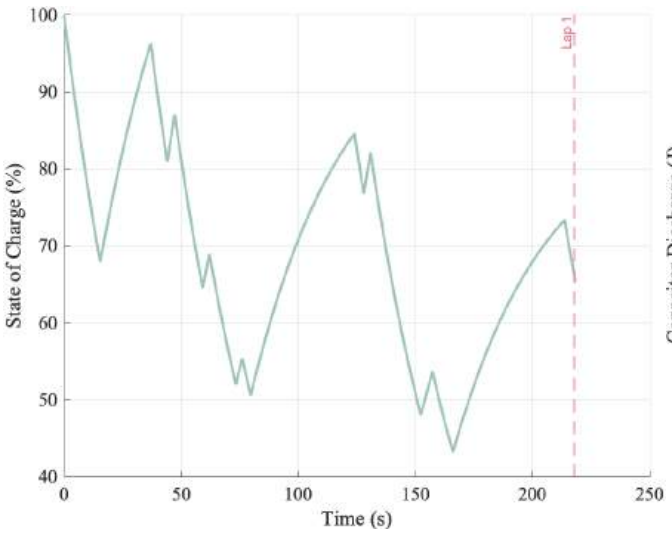


Figure 77: Supercapacitor SOC for 1 Lap.

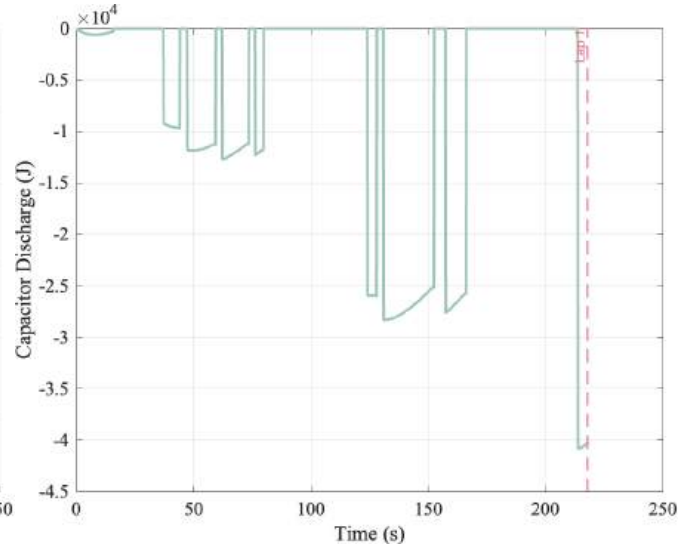


Figure 78: Supercapacitor SOE for 1 Lap.

Figure 77 depicts the supercapacitor SOC against lap time, showing data for a single lap, as estimated by the UCL team's simulation model. The patterns in powertrain behaviour can be seen in Figures 77 and 78. Decreasing SOC indicates pulsing while increasing SOC indicates coasting. Figure 78 depicts the supercapacitor SOE against lap time, which are predictions for a single lap as calculated by the UCL team's simulation model. The energy is negative to indicate capacitor discharge (energy depleted). The energy drops come from the pulsing sections, generating an energy consumption estimate of just under 11kJ per lap, accounting for fuel cell losses.

The race strategy can be analysed using the current deployment around the track. The velocity profile and acceleration dependency for the simulation results are plotted in Figure 79. The important corners are overlaid on the plot to instruct the driver on where the pulsing and coasting regions are.

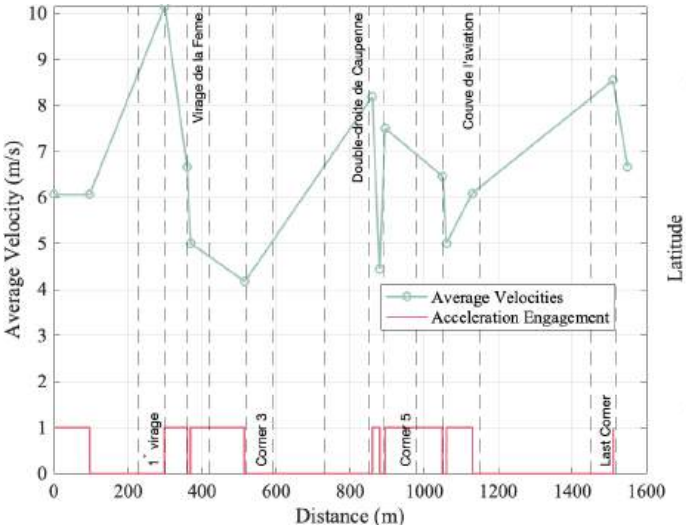


Figure 79: Nogaro Velocity Profile Estimation.

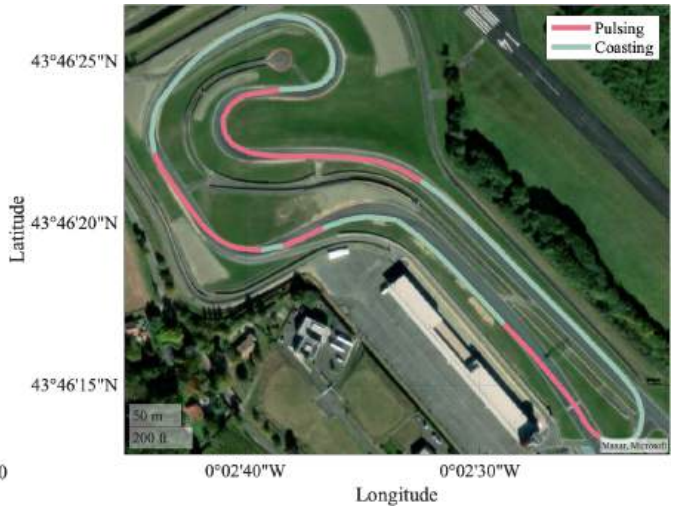


Figure 80: Nogaro Pulsing and Coasting Strategy.

Once the pulsing and coasting distances from the start/finish line have been identified for one lap around Nogaro, they can be mapped on the track's layout. The optimal racing line has been determined using algorithms developed by a Capstone Project member in the previous year's competition which won the Data and Telemetry Award [30]. This took into account the circuit's boundaries to determine the trajectory that minimise the turning curvature in a corner. Figure 80 depicts the new simulation results adapted for the hydrogen car, and its new electrical configuration. This will be used to instruct the driver in their preparation ahead of the competition.

## 5.5 Competition Performance and Results


Figure 81: UCL Shell Eco-Marathon Team winning the Carbon Reduction Footprint at Nogaro Circuit 2024.

The 2024 Shell Eco-marathon competition was a step forward in the UCL team's hydrogen powertrain development. It was the only UK based team to run in the hydrogen class. This category presents considerable challenges in powertrain design to ensure efficiency and safety. The layout of the track includes a steep hill at the start of the race. There were numerous attempts to adjust the powertrain configuration to increase the torque of the car. Unfortunately, due to an issue unrelated to the telemetry system, the team was unable to drive past the hill section to complete the 10 required laps.

During the redesigning and rewiring of the car, the telemetry system proved to be a vital component in monitoring the powertrain. The electrical team used the LCD screen to track the current and voltage readings to ensure that the wiring was correct. The driver interface was adjusted on the spot to prioritise the incoming sensor readings that were requested by the engineers. During the competition attempts, the data storing and wireless communication worked as expected. Unfortunately, as the car did not make it past the pit lane due to the insufficient torque, no meaningful data was collected. In the coming weeks, the data will still be analysed to estimate the deceleration rate and its correlation with the powertrain.

The team's on-going research throughout the season in minimising carbon emissions and reducing energy consumption through data analysis proved to be a major success. Firstly, the UCL team won the Carbon Reduction Footprint Award, climbing once more onto the competition's podium. This work highlighted the team's effort in minimising carbon emission through careful choices of manufacturing and design practices in chassis and powertrain development. Besides this, the importance of data analysis in the identification of race lines that minimise energy consumption was another benefactor to the application.

However, this project's work mainly targeted the Data and Telemetry Award. Due to the innovative solution to identify energy reducing driving strategies and live communication to the driver and race engineer, the award submission scored the highest. This was a great success to the team, which demonstrated the high quality of work and importance of the system to the car development and competition preparation. To be eligible for this award, the car needs to complete a valid attempt at the marathon run. As a result, on this occasion, the award was not won by the UCL team. On the bright side, as the application was out of contention, it can be used the coming season again to reclaim the award title. The telemetry system will remain available to the team and user manuals that contain detailed instructions and a GitHub repository on how to use it have been handed over.

# 6 Design Evaluation and Conclusions

## 6.1 Design Evaluation

With the design complete it can be compared against the FOCs outlined in section 3.1 of the document to determine how successfully it meets the initial design aims. Table 19 shows the FOCs colour coded based on whether they were met (green), partially met (yellow), or not met (red).

As it can be seen most of the design aims were successfully met. However, through the testing of the wireless communication system and after the analysis of the racetrack's geometry it was realised that having continuous radio data communication throughout the track is not possible. This resulted in FOCs 2.2.0 and 2.3.0 not being met, as previously discussed it was realised continuous live data is not necessary for this project. That is why messages are sent in batch. Failure to meet these FOCs also negatively impacted FOC 5.1.2 on the race engineers side. Finally, although the receiver consumes considerably less than 5W making it an ideal choice compared to off the shelf components, with the screen also powered on the overall system's power consumptions goes above 5W, making FOC 6.6.0 partially satisfied.

Table 19: Evaluation of Functions, Objectives, Constraints.
(Green = fully met, Yellow = partially met, Red = not met)

| Function | Objective | Constraint |
|---|---|---|
| **1.0** Data Collection | **1.1.0** Collect relevant data | **1.1.1** All quantities relevant to performance are measured |
| | **1.2.0** Accurate measurements | **1.2.1** Measurement accuracy is within 5% of the actual value |
| | **1.3.0** Prompt measurements | **1.3.1** At least 1 new measurement per second |
| | **1.4.0** Reliable measurements | **1.4.1** The output range for same inputs is within 5% |
| **2.0** Data Transmission | **2.1.0** System sends relevant data | **2.1.1** The relevant data is transmitted to separate interfaces |
| | **2.2.0** Wireless communication | **2.2.1** Data can be sent wirelessly throughout the track |
| | **2.3.0** Continuous data feed into the interfaces | **2.3.1** Data is sent every time a new measurement is processed |
| | | **2.3.2** The data is not delayed more than 200 milliseconds |
| | **2.4.0** Error detection of miscommunication | **2.4.1** Unsuccessful message transfer can be identified |
| | | **2.4.2** Message transfer probability > 90% |
| **3.0** Data Processing | **3.1.0** Raw data decoding | **3.1.1** Raw sensor measurement format |
| | **3.2.0** Prompt data processing | **3.2.1** Raw sensor data should not stockpile |
| | **3.3.0** Low computational intensity | **3.3.1** Processing can be done with microcontrollers |
| **4.0** Data Storage | **4.1.0** Data is stored permanently | **4.1.2** The data is not lost if the storage device is powered off |
| | **4.2.0** Data is easy to access | **4.2.1** Intuitive file structure |
| | **4.4.0** Data can be written quickly | **4.4.1** Data storage does not impact processing times |
| **5.0** Data Visualisation | **5.1.0** Performance data is displayed reliably and accurately | **5.1.1** All necessary information is displayed simultaneously |
| | | **5.1.2** Displayed information is up-to-date |
| | **5.2.0** Interface is intuitive and easy to interpret | **5.2.1** The display layout adheres to the wants of the users |
| | | **5.2.2** Display does not compromise the user's safety |
| **6.0** System Design | **6.1.0** Easy to use | **6.1.1** System can easily be taken apart and assembled |
| | | **6.1.2** No ambiguities regarding its assembly |
| | **6.2.0** Easy to expand | **6.2.1** Developments have to be compatible with current system |
| | **6.3.0** Easy to manufacture | **6.3.1** Manufacturing requirements are easily available |
| | **6.4.0** Sustainable | **6.4.1** Can be recycled |
| | **6.5.0** Low weight | **6.5.1** System is lighter than 1kg |
| | **6.6.0** Low power consumption | **6.6.1** System uses less than 5W |
| | **6.7.0** Low-cost | **6.7.1** System costs < £2500 |
| | **6.8.0** Robust | **6.8.1** Components withstand race conditions |

### 6.2 Conclusions

The development and integration of the live telemetry system for the UCL Shell Eco-marathon team represent a significant achievement in enhancing the team's competitive edge through advanced technological innovation tailored for the competition, which cannot be achieved through existing telemetry systems on the market.

The introduction of modular PCB components have enabled the system to be easily expandable and adaptable to different data collection needs. Effective data transmission paired with robust data processing and storage has significantly improved the team's ability to make informed strategic decisions. In addition, the real time driver interface provides immediate and intuitively feedback to the driver on their performance and the vehicle's state, which helps the driver improve their driving during the race. A live race engineer interface aids the race engineer to evaluate the driver's performance, allowing them to provide feedback for the driver during the race. In terms of protective casings, these were optimised for minimum weight and user-friendliness. Moreover, the project has laid a solid foundation for future enhancements. The telemetry system's flexible architecture allows for easy integration of new sensors and modules, ensuring that it can evolve with advancing technologies and changing team needs. This adaptability is crucial for maintaining technological relevance and a competitive advantage in the future. Most importantly, the design solution has satisfied most of the FOCs stated in Table 19.

The team applied for the 2024 Shell Eco Data and Telemetry award using this project and scored 88 out of 100, which was the highest score amongst all teams. This accomplishment not only highlights the system's innovations but also demonstrates Shell's confidence in the idea. The high score also reflects the effectiveness of the solution in addressing the engineering problem's requirements and positions the UCL Shell Eco-marathon team for continued success in its future endeavours.

## 7 Future work

Three aspects of the project could be improved in the future. These are the accuracy, speed, and quantity of parameters being measured, the data structure to store the recorded measurements, and the accuracy of the simulations.

### 7.1 Filtering

Filtering combines multiple sensor readings to create a more accurate and frequent reading. There are various types of filters, the simplest one to implement is the complementary filter [31]. However, most applications utilise the Kálmán filter [32, 33]. The current system allows for the combination of high frequency but less accurate IMU readings with low frequency but accurate GPS readings for better velocity and position readings.

### 7.2 Hydrogen Flow-meter Integration

The current hydrogen flow-meter owned by the team is not compatible with CAN. Due to the hydrogen powertrain being completed close to the final stages of the project, there was insufficient time to provide a reliable solution to incorporate a flow-meter needed for the hydrogen car. This would allow the team to evaluate how much energy is lost in converting the hydrogen into useful energy to identify further energy losses and areas of improvement.

### 7.3 Online Database

Currently, vehicle data is being stored locally on an SD card as text files. Although this approach meets the requirements of the project, it can be further improved by using a database to store the sensor values. This makes them easier to filter and analyse. Furthermore, an online database could be implemented to which the vehicle continuously sends data wirelessly. This would allow for multiple people to access the data in real-time independent of location.

### 7.4 Digital twin

Using the data gathered by the system along with machine learning, a digital twin could be created. This allows the team to do preliminary tests virtually. This would greatly reduce the team's carbon footprint since the car would not need to be transported to the test site along with the team.

# References


[1] Geraint Rees Carol Paige Michael Arthur, Fiona Ryland. The strategy for a sustainable ucl, 2024.

[2] Yomna Noor El-Deen Abdullah Al Majali Aadil Johnson Omar Gharaibeh, Saif Siddiki. Shell Eco-Marathon: UCL Team Hydrone, 2015.

[3] Rajan Rai-Ahmed Khalil Stefanos Ziomas Jason Biddlecombe Daniel Wheller Stephane Couvreur Tinius Bierman, Ingvild Steen Peersen. UCL Racing shell Eco Marathon Hydrone AB4, 2017.

[4] German Lee Dimitrios Pavlides Marios Pentheroudakis Nicolas Thorel Simon Frearson, Carmen Salvadores. University Colllege London - Shell Eco-Marathon 2019, 2019.

[5] Jörge Segers. Analysis techniques for racecar data acquisition, 2nd edition. *ProtoView*, 1(18), 2014.

[6] EE Times Asia. Critical electronics in formula 1 race cars. `https://www.eetasia.com/critical-electronics-in-formula-1-race-cars/`, 2023. Accessed: 2023-04-15.

[7] Kirsten Matheus and Thomas Königseder. *Automotive ethernet / Kirsten Matheus, Thomas Königseder.* Cambridge University Press, Cambridge, third edition. edition, 2021.

[8] K. Etschberger. *Controller Area Network: Basics, Protocols, Chips and Applications.* IXXAT Press, 2001.

[9] Dominique. Paret. *FlexRay and its applications : real time multiplexed network / Dominique Paret.* Wiley, Hoboken, NJ, 2012.

[10] *IEEE Standard for Local Area Networks : Token Ring Access Method and Physical Layer Specifications / IEEE.* IEEE Std ; 802.5-1989. IEEE, New York, N.Y, 1989.

[11] Rainer König and Christian Thiel. Media oriented systems transport (most®) - standard für multimedia networking im fahrzeug / media oriented systems transport - standard for multimedia networking in vehicle environment. *Information technology (Munich, Germany)*, 41(5):36–43, 1999.

[12] Tim Keary. 6 best network topologies explained - pros & cons [includes diagrams], 2024. Accessed: 2024-04-16.

[13] Christopher Brown. *Making sense of squiggly lines : the basic analysis of race car data acquisition / written by Christopher Brown.* Christopher Brown Racing, California, USA, 1st edition. edition, 2011 - 2011.

[14] Simon Hainz, Elisa de la Torre, and Johannes Güttinger. Comparison of magnetic field sensor technologies for the use in wheel speed sensors. In *2019 IEEE International Conference on Industrial Technology (ICIT)*, pages 727–731, 2019.

[15] As easy as a.b.s, 2024. Accessed: 2024-04-16.

[16] Throttle position sensors (tps), 2024. Accessed: 2024-04-16.

[17] What is an accelerometer: Definition, types and applications, 2022. Accessed: 2024-04-16.

[18] Jetmir Haxhibeqiri, Eli De Poorter, Ingrid Moerman, and Jeroen Hoebeke. A survey of lorawan for iot: From technology to application. *Sensors (Basel, Switzerland)*, 18(11):3995–, 2018.

[19] Shahin Farahani. *ZigBee Wireless Networks and Transceivers.* Elsevier Science, San Diego, 1 edition, 2011.

[20] Bill Flerchinger, Robert Ferraro, Chris Steeprow, Michael Mills-Price, and J. W. Knapek. Field testing of 3g cellular and wireless serial radio communications for smart grid applications. In *2016 IEEE Rural Electric Power Conference (REPC)*, volume 2016-, pages 42–49. IEEE, 2016.

[21] Dimas Tribudi Wiriaatmadja and Kae Won Choi. Hybrid random access and data transmission protocol for machine-to-machine communications in cellular networks. *IEEE Transactions on Wireless Communications*, 14(1):33–46, 2015.

[22] imc Test Measurement GmbH. Technical data sheet: Dx - digital multi-channel telemetry system. ://www.imc-tm.com/download-center/product-downloads/dx-telemetry/data-sheets.

[23] InHand Networks. Invehicle g710 datasheet. https://www.hy-line-group.com/products/hcp/datasheet/inhand/invehicle-g710-datasheet.pdf, 2024. Accessed: 2024-05-22.

[24] Autotel. Autotel product datasheet. https://www.autotel.co.uk/index.php?route=product/product/download&document_id=92, 2024. Accessed: 2024-05-22.

[25] Sam Broyles. A system evaluation of can transceivers, 2022.

[26] Norman Koch. *Shell Eco-Marathon 2024 Official Rules Chapter I.* Shell Eco-Marathon, Carel van Bylandtlaan 30, 2596 HR The Hague, The Netherlands, 3rd edition, September 2024. Available at https://www.shellecomarathon.com/about/global-rules.html.

[27] Katharina Battes, Christian Day, and Volker Hauer. Outgassing behavior of different high-temperature resistant polymers. *Journal of Vacuum Science and Technology*, 36(2):1–2, 2017.

[28] Nesnes. Teleplot: Ridiculously-simple telemetry viewer. https://github.com/nesnes/teleplot, 2024.

[29] George Stonor. Building a model of the michelin 35-406 tyre, 2023.

[30] Albert Cristian Tanase. Computational modelling and simulation of the 2023 shell eco-marathon car, 2023.

[31] Parag Narkhede, Shashi Poddar, Rahee Walambe, George Ghinea, and Ketan Kotecha. Cascaded complementary filter architecture for sensor fusion in attitude estimation. *Sensors*, 21(6), 2021.

[32] Maciej Salwa and Izabela Krzysztofik. Application of filters to improve flight stability of rotary unmanned aerial objects. *Sensors*, 22(4), 2022.

[33] OlliW. IMU Data Fusing: Complementary, Kalman, and Mahony Filter, 2013.